Response to interactive comments to the Discussion paper:

“Extracting information on the spatial variability in erosion rate stored in detrital cooling age distributions in river sands” by Braun et al.

Reviewer #1’s comments

This section needs some improvements and reference to previous work, in order to properly emphasize the complexities of the thermochronologic record and the main assumptions of the detrital thermochronology approach (see below):
1) "Thermochronometric methods provide us with estimates of the cooling age of a rock, i.e. the time in the past when the rock cooled through a so-called closure temperature (Dodson, 1973), which varies between systems and minerals."
The concept of a closure temperature and a cooling age only applies in the case where rocks are cooling monotonically from high to low temperature (e.g., Dodson 1973; Villa 1998). For example, if a rock cools rapidly into the partial retention zone and is resident therein for a period of time before cooling again, its thermochronologic age cannot be recognized as a "cooling age". It is a common assumption in detrital thermochronology studies that all ages represent cooling ages, but this is not necessarily the case. This assumption should be properly underlined in the revised main text.
We have change the sentence.
2) "One of the main geological processes through which rocks experience cooling is exhumation towards the cold, quasi-isothermal surface (Brown, 1991)."
I would underline here that the thermal reference frame relevant for isotopic closure is generally dynamic, which makes the interpretations of thermochronologic ages even more challenging, especially in detrital thermochronology.
We don’t fully understand the comment by the reviewer, i.e. what he means by “generally dynamic”.
3) "Young ages are commonly interpreted to indicate rapid exhumation and old ages should correspond to slow exhumation."
Old ages can also reflect denudation of shallow crustal levels that lay above the isothermal surface corresponding to the closure temperature of the thermochronologic system under consideration (e.g., Rahl et al. 2007).
We have rewritten this sentence to make it clearer.
4) "Cooling ages can also record more discrete cooling events such as the nearby emplacement of hot intrusions (Gleadow and Brooks, 1979) or the rapid relaxation of isotherms at the end of an episode of rapid erosion (Braun, 2016)."
A similar interpretation as Braun (2016) was also proposed for the European Southern Alps by Zanchetta et al. 2015 - Lithosphere. Cooling ages can also record thermal relaxation during the rifting to drifting transition (Malusà et al. 2016a - Gondwana Research), or mineral crystallization that has occurred at shallow crustal depth above the closure temperature isothermal surface (e.g., Malusà et al. 2011 - EPSL).
We have added appropriate references.
5) "Datasets are now routinely assembled by collecting and dating a large number of mineral grains from a sand sample collected at a given location in a river draining

an actively eroding area. Such detrital thermochronology datasets provide a proxy for the distribution of surface rock ages in a given catchment (Bernet et al., 2004; Brandon, 1992)"
This only applies in case of uniform mineral fertility in eroded rocks (Malusà et al. 2016b - Gondwana Research).
We have rewritten this sentence and added a small discussion on the importance of estimating what we refer to as mineral surface concentration factors and the reviewer calls “fertility”.
6) "By repeating this operation at different sites along a river stream, one obtains redundant information that can be used to document more precisely the spatial variability of in-situ thermochronological ages in a river catchment (Bernet et al., 2004; Brewer et al., 2006)."
The detrital thermochronologic record reflects both the thermochronologic complexities of eroded bedrock, and the bias acquired during erosion, transport and deposition (e.g., hydraulic sorting and mineral fertility bias, see Malusà et al. 2013 - Chemical Geology; Malusà et al. 2016b - Gondwana Research). All of these complexities and potential sources of bias should be properly taken into account and mentioned in the revised main text.
We have include a short paragraph on the importance of the fertility factor mentioned by the reviewer. We have also included a better explanation of what our alpha parameter means, but our paper is not the place to review (and cite) all the literature on the subject. If there are reliable means to estimate the fertility bias, anyone using our proposed method should, of course, use it. But it is not the purpose of our paper to enter into this discussion.
7) "However, these methods have not taken advantage of the fact that detrital age distributions contain two separate pieces of information concerning the spatial patterns of present and past rates of erosion. The first piece of information comes from the ages themselves: catchments or sub-catchments where the proportion of grains with young ages dominates are likely to experience rapid exhumation today or in the recent past; whereas catchments or sub-catchments where the proportion of grains with old ages dominates are more likely to have experienced rapid erosion in a more distant past."
This is not novel. The dual information (long-term vs short-term erosion/exhumation) provided by detrital thermochronology datasets was first discussed by Malusà et al. 2009 (Geol Soc London Spec Publ) under the assumption of constant mineral fertility in the eroding sources. This topic was further developed by Resentini and Malusà 2012 (Geol Soc Spec Papers) and Malusà et al. 2016b (Gondwana Research), taking into account the dishomogeneous mineral fertility in the source rocks. All these papers should be quoted in the revised manuscript.
We have cited the work by Resentini and Maulsa 2016b which uses a similar, yet different method. In their analysis they assume that they know to which peak(s) in the age distributions each of the subcatchment contributes to (similar to assuming the relative values of the Cik in our method; see Figure 8 in Resentini and Malusa 2016)
8) "In each Area i, we will assume that alpha i is the relative abundance of the mineral used to estimate the age distribution in rocks being eroded from the

surface. We take the convention that 0 < alpha i < 1, with alpha i = 1 corresponding to an area i with surface rocks that contain the mineral in abundance (for example granite for muscovite) and alpha i = 0 corresponding to an area i with surface rocks that do not contain the mineral (for example carbonates for muscovite). If, for example, the area is made of 60% granite and 40% carbonates, and we have measured ages using a mineral that is abundant in granites (like muscovite) but absent in carbonates, then alpha = 0.6."
Alpha just provides a rough estimate of the mineral fertility bias. Malusà et al (2016b) demonstrated that major mineral fertility variations can be observed even in tectonic units with similar lithology, and showed that the relationships between bedrock geology and mineral fertility are complex and hardly predictable. They depend not only on lithology, but more in general on the whole magmatic, sedimentary or metamorphic evolution of eroded rocks. Careful approaches to mineral fertility measurements are consequently required (see Malusà et al. 2016b - Gondwana Research). I think that this issue should be discussed in more detail in the revised manuscript.
As stated earlier, we have added a paragraph on mineral fertility bias .
9) "Table 2" The lithological factor shown in Table 2 is very similar for different catchments. Is this correct? Was the mineral fertility measured accurately? Expected mineral fertility variations in Alpine-type orogenic belts should be on the order of 10e2-10e3 (see, e.g., Malusà et al. 2016b - Gondwana Research).
In the application of our method to the Eastern Himalaya dataset, we have compared results obtained by using uniform values for the alpha parameters to those obtained by using first-order estimates of the alpha parameters derived from the geological map. Although the results are dependent on this choice, the most salient feature of the results (large increase in erosion rate near the syntaxis) is not affected.
10) "Interestingly, there is a good correspondence between present-day erosion rate C4 and where the youngest ages are being generated (compare upper left panel showing relative concentration of youngest age bin, to central panel showing predicted present- day erosion rate), with the notable exception of the most downstream catchment (Z). In other words, where the mixing analysis predicts high erosion rate to account for a substantial change in the age distribution between two adjacent catchments, is also where it predicts the highest concentration of young ages in the surface rocks."
The short-term erosion rates calculated by Braun et al. are strongly influenced by the mineral fertility bias. Without an accurate measurement of mineral fertility and a proper consideration of hydraulic sorting effects, the comparison between long-term and short-term erosion rates performed here is rather weak.
We have shown how the uncertainty on the alpha parameters influences the accuracy of the estimates of erosion rates.

Reviewer #2's comments

Review of "Extracting information on the spatial variability in erosion rate stored in detrital cooling age distributions in river sands", by Jean Braun, Lorenzo Gemignani,

and Peter van der Beek For consideration for Earth Surface Dynamics.
Recommendation This paper provides an approach for decomposing erosion rates from detrital cooling ages collected from multiple tributaries. The approach is innovative but the quantitative formulation is difficult to follow and the implementation has major problems that undermine confidence in the results. To be blunt, I have no idea if the proposed formulations give the “right answer”. I highlight these problems in my general comments below, and I follow with some specific comments. The paper is not suitable for full publication in its present form, but I think some careful revisions could transform the paper into an important contribution.
General Comments (see Specific Comments below for more details)

1) The paper starts out with a clever idea, to use detrital cooling ages from multiple tributaries to resolve relative modern erosion rates for each of the tributaries. The starting point is excellent.
2) The paper claims to be the first to use detrital thermochronometric data as a tracer for estimating modern erosion rates. This tracer approach has already been introduced by McPhillips and Brandon (2010) and Ehlers et al. (2015). The specific contribution here, using detrital thermochronology as a tracer from multiple nested catchments, is a new and important.
We have added a reference to McPhillips and Brandon (2010)
3) There is actually a lot of literature on the formulation and solution of mixing models. I would expect a brief summary of that literature, and also some discussion about advantages and disadvantages of previous methods and the new method presented in the paper. One analysis that I like is in Menke (2013, p. 10-11, 189-199).
Our method assumes that ages represent distinct events that can be used to define age bins that are then used as tracers. To define those bins, one can construct kernel density estimates of the age distributions. A short sentence has been added to explain this. Alternatively, one could also use the ages distributions to construct estimates of cumulative density functions (CDFs) that could then be used to estimate the minimum required erosion rate to explain differences between two successive CDFs. After testing on synthetic datasets, we have tentatively concluded that such a method is, however, less accurate. This is reported in a new section entitled “Ways in which the method could be improved”.
4) The main contribution of this paper is a computation procedure that uses observed detrital cooling ages collected from tributary catchments and along the trunk stream of a large drainage to estimate average relative erosion rates for each of the tributary catchments. In other words, the estimation involves inverting the data to find best-fit solutions (expectations and confidence intervals) for the relative erosion rates. Inverse estimation is a well-established field and it makes sense to structure the problem in terms of this methodology. To do so requires a clear definition of the model equation and error function, and the determination of a computation method to optimize the unknown parameters relative to the observed data, using either least squares or likelihood. The estimation suggested in the paper provides no tie to statistical or inverse methodology, so it is difficult to know if the

estimates will be correct.

We have lengthened and improved the description of the method and attempted to make it clearer and more rigorous.

5) The paper lacks any testing of the estimation method. The usual approach is to design a synthetic data set with noise, and use that to see if the estimation method recovers the parameters used to generate the synthetic data set. A successful test would show that as the size of the synthetic observed data is increased, the parameter estimates would asymptotically approach the "true" parameter values used to generate the synthetic dataset. I encourage this kind of test to be added to the paper.

We have include a demonstration of the accuracy and usefulness of the method using synthetic data. In particular we have highlighted the importance of having different "age signatures" in different catchments to obtain good estimates of the relative erosion rates.

6) I don't know why, but the authors decide that they can estimate the best-fit result and the uncertainties using a Monte Carlo simulation. They refer to this simulation as a "boot strap" estimation of uncertainties, but that is incorrect (see specific comment #4 below). In fact, they are using this simulation to estimate both the expectations and the uncertainties for the parameters. They note that they prefer the modes, and not the means, of the Monte Carlo distributions as estimators for the relative erosion rates. I understand their preference in that the Monte Carlo distributions are asymmetric, but they provide no evidence to show that the modes or the means work at all. In the end, it would make sense to solve the inverse problem directly, rather than rely on Monte Carlo distributions. Note that the bootstrap method is very useful non-parameteric method for estimating uncertainties. For the problem here, it probably makes sense to estimate bootstrap confidence intervals (see Carpenter and Bithell, 2000 for details), which require no assumptions about the shape of the bootstrap distribution.

We are now showing median values of the distributions obtained by bootstrapping, as well as lower and upper quartiles. This is based on comparing the model results with known erosion rates in the synthetic examples that suggests that median values are most appropriate.

7) There is no discussion of the structure of this estimation problem. Is it overdetermined, underdetermined, or mix determined? One is left to wonder if the constraints (eqs. 15, 16) are handled in a way that is consistent and unbiased with respect to the estimation problem. What is the structure of the errors, and how are the errors accounted for in the estimation algorithm? There is a vagueness about the estimated quantities, whether they are absolute or relative erosion rates. This point should be stated upfront and maintained in consistent way throughout the paper.

The problem is underdetermined. We have shown however, that we can obtained minimum values for the erosion rates in successive catchments to satisfy observed differences in age distributions between successive catchments. We have improved the manuscript to make this point clearer.

8) It is not clear what quantities are being estimated. In the formulation, it would seem that Ck,i are the primary parameters to be estimated (section 2.4), and the

relative erosion rates are derived from these parameters. The values for Ck,i are bounded to the range [0,1], which means that their range is truncated on both sides. Constraints are introduced in the formulation (eqs. 15, 16) but there is no assurance that this strategy will give the right answer. In statistics, the well established approach is to remove the truncations by transforming the parameters to a new scale. The logit transform is used for parameters that are bound to [0, 1], where logit(x) = ln(x /(1-x). A positivity constraint for erosion rates can be introduced by a log transform. These strategies commonly result in symmetric Gaussian-like distributions for the parameters, which means that the best-fit solution and confidence intervals are typically well defined. The authors have the view that it is somehow better to fit “raw binned age data” (p. 3, line 10), rather than a probability density function. The binned data are not “raw” in that they are smoothed by the box function used for the binning. The topic of kernel density estimation (KDE) was first established in the mid 1950’s has been well defined since about the mid-1980’s. What is clear is that the box function used in estimating a histogram is just one type of kernel function. A Gaussian is a much better kernel function for estimating a density distribution. It would make no difference if one used a histogram versus a density distribution for this problem. Silverman (1986) provides a general review of estimating density functions, Brandon (1996) show an extension of the KDE method for use with grain ages with specified standard errors, and McPhillips and Brandon (2010) show how to combine estimated probability density functions to get a relative density function for tracer thermochronology. All of this approach is completely consistent with the formulations proposed in this manuscript. Note that Vermeesch’s (2012) paper on grain age distributions provides nothing new to this issue of density estimation.

See response to point (3)

9) The authors have an application paper, Gemignani et al, 2017, which was published in August in Tectonics. The paper considered here makes no mention of this paper. It is important to provide some explanation of how that paper relates to this contribution.

We have given reference to the Tectonics paper in the introduction.

Specific Comments

1) p. 2, lines 27-28: The paper states that previous publications have not taken advantage of the ability of thermochronologic data to resolve both past and present erosion rates. In fact, McPhillips and Brandon (2010) was entirely devoted to showing how thermochronology can be used as a tracer to estimate modern erosion rates. Ehlers et al. (2015) also has a similar application.

We have added a reference to McPhillips and Brandon (2010).

2) p. 3, lines 9-10, 29-30: Not clear why bins are better why to represent the density of the data. The authors imply that the bins can be tuned to an ‘event of given “age”’, but there is no explanation about why this capability is important or even desired. In addition, there are the usual questions about histograms: How many bins should be used?, How wide should the bins be?, etc.

See response to point (3)

3) p. 6, Incremental Formulation: This section provides another solution for the estimation problem. It would help if there were some explanation about why a

second approach is needed.
It is the same solution/approach but expressed differently. We have made this point clearer.
4) p. 9, line 12: The numerical estimation is described here as a bootstrap, but the method used is not the bootstrap (Efron and Tibshirani, 1986), but rather an ad-hoc procedure. I am puzzled here because the bootstrap calculation is very simple (replicate data sets produced by random sampling with replacement of the original data set), and it has well defined properties for estimation of uncertainties. In contrast, I have no idea if the ad-hoc procedure used here (randomly removing 25% of the data) is able to provide reliable estimates of uncertainties.
We agree that a bootstrap method should not be removing but replacing samples; we have fixed this.
5) p. 9, line 27: It would help to explain here why the closure temperature for Ar muscovite is cited here, given that this information is not used in the paper.
We have removed the reference to the closure temperature, which, we agree, is irrelevant here.
6) p. 12, fig. 4: The horizontal axes have no tic values or axis labels, and the vertical axes are also unlabeled.
We have improved this figure
7) p. 13, lines 5-9: The estimation method seems to be rather unstable.
Using synthetic ages distributions we have shown the reliability of the method.
8) p. 14, figure 5: This figure is hard to understand. It is my guess that the gray scale represents, not the estimated erosion rate, but rather the estimated relative erosion rate. Is that correct?
The figure has been modified to be clearer.

<u>Associate Editor's comments</u>

I find the manuscript basically acceptable as is. It is of fundamental interest and potentially of broad applicability. I am far from understanding the math details underlying the approach presented, but I trust the authors and future users of the method to deal with this if needed.
I have a few comments/questions that the authors are free to consider.
"The first piece of information comes from the ages themselves: catchments or sub-catchments where the proportion of grains with young ages dominates are likely to experience rapid exhumation today or in the recent past; whereas catchments or sub- catchments where the proportion of grains with old ages dominates are more likely to have experienced rapid erosion in a more distant past."
=> Why would "a catchment with old ages" be interpreted as representing an area of rapid erosion in the past. I thought old ages meant slow erosion. Are you only saying that pulses of rapid erosion can't be resolved by thermochronometric method when ages are old? Hence only catchment with young ages would be able to decipher rapid erosion. Isn't there some bias here?
We have changed the sentence to reflect the point made by the AE.
"For this, ages can be regarded as passive markers (or colors) that inform us on the proportion in which the mixing takes place today, which is directly proportional to

the present-day erosion rate."
=> what is the relation that determines a direct proportionality link between the "mixing of passive markers in a river" and "present-day erosion rate". Is this obvious or are there any references to back this up?
Because faster present-day erosion rate will yield a proportionally larger sediment flux into the river, everything else being considered the same. We have adapted the sentence to avoid the confusion caused to the AE.
"we have devised a simple method that, unlike many others such as that of Brewer et al. (2006), is only dependent on the raw, binned age data." I guess I understand that here you're bypassing the need to model individual age data into cooling rates through assumptions of geothermal gradients etc. . . If that's correct I must say that for a non-specialist it would be great to have a bit more material here on the assumptions that are made and not made.
We have changed the text to make this clearer
Also, are the ages really "raw" or do they come with uncertainty/standard error on them? And if yes, what are the uncertainties/SE on "raw" ages.
In the abstract it is said "We show that detrital age distributions contain dual information about present-day erosion rate" but in the text it is more an assumption than a demonstration. And I also failed to see how the results obtained are confronted with existing constraints on erosion rates in this area.
We have added a paragraph comparing the distribution of erosion rates predicted by our method to previous estimates.
4. Uncertainty estimates. Since the distribution are not normal, does it makes sense to use the standard deviation around the mode? Also, wouldn't it be possible to perform a standard error propagation that would include the standard errors on ages?
We now show how well the method behaves when applied to synthetic ages distributions with finite age uncertainty. This clearly helps identifying the main sources of uncertainty.
Conclusion: thanks to the authors for submitting their work to eSurf and apologies again for the slow process.

Extracting information on the spatial variability in erosion rate stored in detrital cooling age distributions in river sands

Jean Braun[1], Lorenzo Gemignani[2], and Peter van der Beek[3]

[1]GFZ German Research Centre for Geosciences, Telegrafenberg 14473, Potsdam, Germany
[2]Department of Earth Sciences, Vrije Universiteit Amsterdam, De Boelelaan 1083, 1081 HV Amsterdam, The Netherlands
[3] ISTerre, Université Grenoble Alpes, CS 40700, 38058 Grenoble Cedex 9, France

Correspondence to: J. Braun (jbraun@gfz-potsdam.de)

Abstract. ~~The purpose of~~ One of the main purposes of detrital thermochronology is to provide constraints on regional scale exhumation rate and its spatial variability in actively eroding mountain ranges. Procedures that use cooling age distributions coupled with hypsometry and thermal models have been developed in order to extract quantitative estimates of erosion rate and its spatial distribution, assuming steady state between tectonic uplift and erosion. This hypothesis precludes the use of these procedures to assess the likely transient response of mountain belts to changes in tectonic or climatic forcing. Other methods are based on an a priori knowledge of the in-situ distribution of ages to interpret the detrital age distributions. In this paper, we describe a simple method that, using the observed detrital mineral age distributions collected ~~in a system of rivercatchments~~along a river, allows to extract information about the relative distribution of erosion rates in an eroding ~~hinterland~~ catchment without relying on a steady-state assumption~~or~~, the value of thermal parameters, or an a-priori knowledge of in-situ age distributions. The model is based on a relatively low number of parameters describing lithological variability among the various ~~catchments~~ sub-catchments and their sizes, and only uses the raw ~~binned ages.~~ ages. The method we propose is tested against synthetic age distributions to demonstrate its accuracy and the optimum conditions for it use. In order to illustrate the method, we invert age distributions collected along the main trunk of the Tsangpo-Siang-Brahmaputra river system in the Eastern Himalaya~~, one of the most tectonically active places on Earth~~. From the inversion of the cooling age distributions we predict present day erosion rates of the catchments along the ~~Siang-Tsangpo-Brahmaputra~~ Tsangpo-Siang-Brahmaputra river system, as well as ~~smaller~~ some of its tributaries. We show that detrital age distributions contain dual information about present-day erosion rate, i.e. from the predicted distribution of surface ages within each catchment and from the relative contribution of any given catchment to the river distribution. The ~~inversion~~ method additionally allows comparing modern erosion rates to long-term exhumation rates. We provide a simple implementation of the method in ~~R.~~Python code within a Jupyter Notebook that includes the data used in this paper for illustration purposes.

1 Introduction

Thermochronometric methods provide us with ~~estimates of the cooling age~~ information pertaining to the cooling history of a rock. Various systems and minerals provide information on different parts of that cooling history, i.e. ~~the time in the past when the rock cooled through a so-called closure temperature (Dodson, 1973), which varies between systems and minerals~~at a given temperature but more commonly within a range of temperatures. One of the main geological processes through which rocks experience cooling is exhumation towards the cold, quasi-isothermal surface (Brown, 1991). Young ages are commonly interpreted to indicate ~~rapid exhumation and old ages should correspond to~~ recent or rapid exhumation whereas old ages usually correspond to ancient or slow exhumation. Cooling ages can also record more discrete cooling events such as mineral crystallization during melt solidification, the nearby emplacement of hot intrusions (Gleadow and Brooks, 1979) or the rapid relaxation of isotherms at the end of an episode of rapid erosion ~~(Braun, 2016)~~(Kellett et al., 2013; Braun, 2016).

~~Datasets are now routinely assembled by collecting and dating~~ Besides collecting in-situ data, one can also collect and date a large number of mineral grains from a sand sample collected at a given location in a river draining an actively eroding area. Such detrital thermochronology datasets provide a proxy for the distribution of surface rock ages in a given catchment (Bernet et al., 2004; Brandon, 1992). By repeating this operation at different sites along a ~~river~~ trunk stream, one obtains redundant information that can be used to document more precisely the spatial variability of in-situ thermochronological ages in a river catchment (Bernet et al., 2004; Brewer et al., 2006).

Methods have been devised to extract quantitative information from such detrital datasets concerning the erosion history of a tectonically active area, as well as estimates of its spatial variability. Ruhl and Hodges (2005) convolved their detrital age datasets with the hypsometry of the catchment to test the assumption of topographic steady-state in a rapidly eroding catchment of Nepalese Himalaya. Similarly, Stock et al. (2006) and Vermeesch (2007) combined detrital apatite (U-Th)/He age datasets with an age-elevation relationship established from in-situ samples to predict the distribution of present-day erosion rates in the eastern Sierra Nevada and White Mountains of California, respectively. Whipp et al. (2009) used simulations from a thermo-kinematic model to define the limits of applicability of such a technique, while Enkelmann and Ehlers (2015) used it in a glaciated landscape. Wobus et al. (2003, 2006) collected samples from tributaries of the Burhi Gandaki and Trisuli rivers to document the strong transition in erosion rate across a major topographic transition. By limiting their sampling to tributaries, they circumvented the need to develop and use a mixing model for the interpretation of their data. Brewer et al. (2006) derived optimal values for erosion rate in neighbouring catchments by comparing and mixing theoretical probability density distributions with detrital age data from the Marsyandi River in Nepal. ~~More recently,~~ Resentini and Malusà (2012) used a similar approach to interpret data from the Western Alps. McPhillips and Brandon (2010) used detrital cooling ages combined with in-situ age measurements to infer a recent increase in relief in the Sierra Nevada, California.

~~However, these methods have not taken advantage of the fact that detrital age distributions contain two separate pieces of information concerning the spatial patterns of present and past rates of erosion. The first piece of information comes from the ages themselves: catchments or sub-catchments where the proportion of grains with young ages dominates are likely to experience rapid exhumation today or in the recent past; whereas catchments or sub-catchments where the proportion of grains~~

with old ages dominates are more likely to have experienced rapid erosion in a more distant past. However, there does not need to be a one-to-one correlation between young ages and fast present-day erosion rate or old ages and low present-day erosion rate, as a rapidly exhuming catchment may not have experienced sufficient total erosion to exhume rocks bearing reset ages. Alternatively regions that produce relatively young ages may have experienced a step decrease in erosion rate in the recent past.

The second source of information comes from the mixing that takes place All of these methods rely on a-priori knowledge or hypotheses concerning the age distributions in the catchments drained by the river from which the samples have been collected. Here we explore the possibility of deriving first-order information about the spatial variability of erosion rate in the river . For this, ages can be regarded catchment when no such knowledge exists and without making any assumption concerning the spatial distribution of ages. We propose to regard ages as passive markers (or colorstracers) that inform us on the proportion in which the mixing takes place today, which is must be directly proportional to the present-day erosion rate. Using this information, the fastest For example, the most rapid present-day erosion rates should be predicted where the age distributions change the most rapidly along the river/stream, everything else being accounted for, such as the relative size of neighbouring neighboring sub-catchments or the potential change in lithology between them. Here we propose that combining the two sources of information should tell us more about the present-day erosion rate and, as we will show, about its antiquity. This knowledge about the distribution of erosion rates, which is obtained independently of the absolute values of the ages, can be used to estimate the distribution of ages in each sub-catchment drained by the river. This second piece of information provides additional insight into the spatial distribution of past cooling/erosional events.

To demonstrate this point, we have devised a simple method that , unlike many others such as that of Brewer et al. (2006), is only dependent In this paper, we present a method that relies on the raw , binned age data age data only. This avoids any complication or bias that may arise from trying to compare the data to theoretical probability density distributions that rely on a thermal model prediction. We recognise recognize the value of doing so, but thermal models require making assumptions about past geothermal gradient (heat flux), or rock thermal conductivity and heat production, which introduces additional uncertainty in interpreting the data. The first part of this paper describes the method.

Due to its relative simplicity, our method is, however, strongly limited by the quality and representativeness of the measured age distributions, i.e. whether samples of 30 to 100 grains are representative of the age distribution of an entire catchment. To test the robustness of our predictionsTo demonstrate its accuracy and explore the limits of its applicability, we have used a simple bootstrapping algorithm that yields uncertainty estimates on the derived erosion ratesapplied the method to synthetic age datasets for which we know the erosion rate and its spatial variability. This is briefly explained done in the second part of the paper.

To demonstrate the ease of use , applicability and usefulness of our new To illustrate the use of our method, we have applied it to several datasets a dataset collected in the Himalaya (along the Tsangpo-Siang-Brahmaputra river system). This is explained in the third part of the paper. There we show that the method yields reliable estimates of the distribution of present-day erosion rates in these areas as well as independent information on the spatial extent of past geological events. We conclude by suggesting potential ways in which the method could be improved. Note that the approach proposed here

has been used on a set of detrital age distribution collected along the Inn River in the Eastern Alps (Gemignani et al., 2017). Gemignani et al. (2017) showed how age distributions characterized by young age peak likely produces high estimates of present day erosion rates when compared with catchments that contain older age peaks.

2 The method

2.1 Basic assumptions

We assume that we have collected a series of age datasets measured at M specific points (or sites) along a river that drains a tectonically active regions where erosion rate is likely to vary spatially. We also assume that the datasets have been used to construct ~~ages~~ age distributions decomposed into N age *bins* (see Figure 1) that may, for example, correspond to given, known geological events or, alternatively, have been selected ~~without prior knowledge, usually uniformly distributed and of equal age width over a given age range, i.e. the range of observed ages (see Figure 1)~~after constructing a Kernel Density Estimate of the data (Vermeesch, 2012) and applying a mixture model to infer potential discrete age peaks in the age distribution (Sambridge and Compston, 1994). Although each bin corresponds to an age range, it might be easier to refer to it as representative of ~~an event of~~ a given "age", which can be taken as the mean age of the range, for example. We will call H_i^k for $k = 1, \cdots, N$ and $i = 1, \cdots, M$ the relative height of bin k in distribution i. Because these are relative contributions, we have:

$$\sum_{k=1}^{N} H_i^k = 1, \quad \text{for all } i = 1, \cdots, M \tag{1}$$

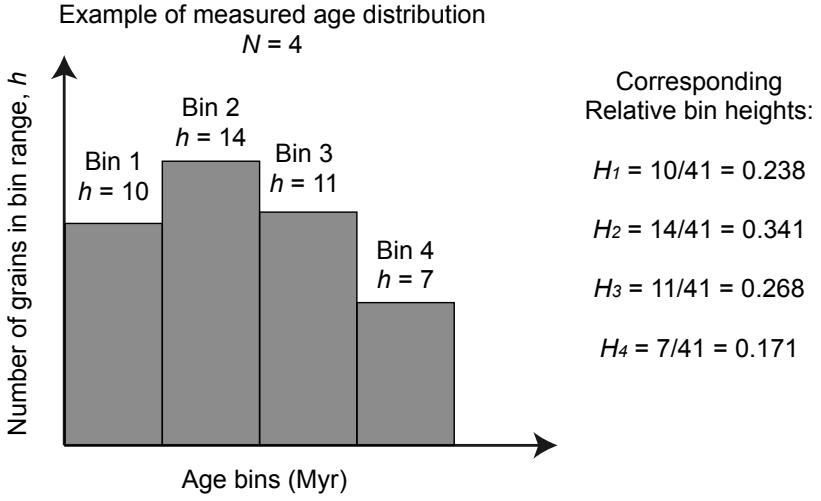

Figure 1. Example of a measured age distribution and the relative heights H_i^k of the corresponding bins ($N = 4$ in this example).

The landscape is divided into *exclusive* contributing areas for each of the points along the main river where we have measured a dataset and compiled ~~from it a distribution~~ a distribution from it. We take the convention that Area 1 (of surface area A_1) is the area contributing to site 1, whereas Area 2 (of surface area A_2) is the area contributing to site 2 but not to site 1. Area i (of surface area A_i) therefore contributes to site i but not to the previous $i-1$ sites (see Figure 2). In each Area i, we will assume that α_i is the relative abundance of the mineral used to estimate the age distribution in rocks being eroded from the surface. We will call α_i the "mineral concentration factor" of Area i. We take the convention that $0 < \alpha_i < 1$, with $\alpha_i = 1$ corresponding to an area i with surface rocks that contain the mineral in abundance ~~(for example granite for muscovite)~~ and $\alpha_i = 0$ corresponding to an area i with surface rocks that do not contain the mineral~~(for example carbonates for muscovite). If, for example, the area is made of 60% granite and 40% carbonates, and we have measured ages using a mineral that is abundant in granites (like muscovite) but absent in carbonates, then $\alpha = 0.6$~~. We also call ϵ_i the unknown present-day mean erosion rate in Area i.

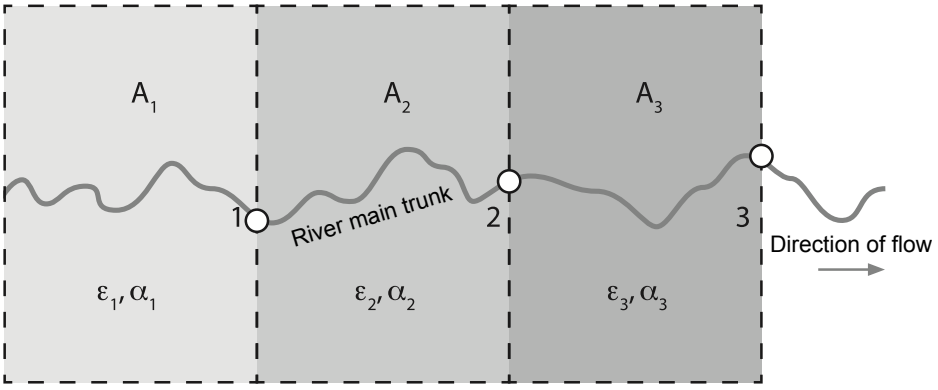

Figure 2. Schematic representation of how the landscape is divided into exclusive contributing areas A_i (different shades of grey) for each of the points (here the circles labeled $i = 1, \cdots, 3$) along the main river where we have age distributions. ϵ_i and α_i are the assumed mean erosion rate and ~~surface rock~~ mineral ~~density~~ concentration factor of ~~area~~ Area i, respectively.

The surface areas, A_i, can be computed from a Digital Elevation Model. The value of the concentration factors ~~is critical; constraining them~~ depends on the regional geology~~and available data. A first-order approximation of the concentration factors or 'fertility',~~. First-order estimates of the α_i ~~,~~parameters can be derived ~~from a geological map or from the relative concentration of given minerals in each of the samples used to derive the age distributions, by using the method described in Malusà et al. (2016), for example~~by considering the relative occurrence of the specific mineral bearing rocks in each area from a geological map. However, recent work shows that mineral abundance in river sediments can vary significantly between tectonic units with similar lithology (Malusà et al., 2016). In their work, Malusà et al. (2016) propose a quantitative approach that can be used to infer potential "mineral fertility" bias between adjacent catchments and provide an example from the Alps. It is not the purpose of this paper, however, to speculate on the bias induced by the mineral fertility parameter in the interpretation of detrital age distributions. We refer to previous work such as that of Malusà et al. (2016) or Resentini and Malusà (2012) on the subject and

assume that if the necessary data is available to perform a correction for this bias, it should be made by adjusting the value of the mineral concentration factor α_i accordingly.

From these simple assumptions, we can ~~then~~ write that the number of grains of age k coming out of catchment i is given by:

$$D_i^k = A_i \alpha_i \epsilon_i \alpha_i C_i{}^k = F_i \epsilon_i C_i^k \tag{2}$$

where $F_i = A_i \alpha_i$ and C_i^k is the unknown relative concentration of grains of age k in surficial rocks in Area i. We also have:

$$\sum_{k=1}^{N} C_i^k = 1, \quad \text{for all } i \tag{3}$$

because the C_i^k are also relative or normalized concentrations. The relative concentrations, C_i^k tells us ~~if the event corresponding to~~ to what extent age k has ~~affected Area i (or, more correctly, if it has~~ been preserved in ~~its surficial rocks)~~ surficial rocks of Area i, whereas ϵ_i is a measure of present-day erosion rate in Area i.

2.2 Downstream bin summation along main trunk

We can now write that the predicted height of bin k in the distribution observed at site i should be equal to the total number of grains of ~~age bin~~ age-bin k coming from all upstream areas divided by the total number of grains of all ages coming from all upstream areas:

$$H_i^k = \left(\sum_{j=1}^{i} D_j^k\right) / \left(\sum_{k=1}^{N}\sum_{j=1}^{i} D_j^k\right) = \left(\sum_{j=1}^{i} A F_j \epsilon_j \alpha_j C_j^k\right) / \left(\sum_{k=1}^{N}\sum_{j=1}^{i} A F_j \epsilon_j \alpha_j C_j^k\right) \tag{4}$$

We can slightly re-arrange this to obtain:

$$H_i^k = \left(\sum_{j=1}^{i} A F_j \epsilon_j \alpha_j C_j^k\right) / \left(\sum_{j=1}^{i} A F_j \epsilon_j \alpha_j \sum_{k=1}^{N} C_j^k\right) = \left(\sum_{j=1}^{i} A F_j \epsilon_j \alpha_j C_j^k\right) / \left(\sum_{j=1}^{i} A F_j \epsilon_j \alpha_j\right) \tag{5}$$

If we divide the numerator and denominator of this expression by ~~$A_1 \epsilon_1 \alpha_1$~~ $F_1 \epsilon_1$, we obtain:

$$H_i^k = \sum_{j=1}^{i} \rho_j C_j^k \Big/ \sum_{j=1}^{i} \rho_j \tag{6}$$

where:

$$\rho_j = \frac{A_j \epsilon_j \alpha_j}{A_1 \epsilon_1 \alpha_1} \frac{F_j \epsilon_j}{F_1 \epsilon_1} \tag{7}$$

is the contribution from Area j relative to Area 1. Note that, if we assume that we can confidently estimate ~~A_j and α_j~~ $F_j = A_j \alpha_j$, ρ_j becomes a measure of the unknown erosion rate, ϵ_j, in Area j relative to the unknown erosion rate, ϵ_1, in Area 1.

2.3 Incremental formulation

We now ~~try to~~ express Equation (6) as an incremental relationship between H_i^k and H_{i-1}^k only, i.e. between the relative bin heights ~~between~~ of distributions measured at two successive points along the main trunk. From Equation (6), we can write:

$$H_i^k = \sum_{j=1}^{i} \rho_j C_j^k / \sum_{j=1}^{i} \rho_j = \left(\sum_{j=1}^{i-1} \rho_j C_j^k + \rho_i C_i^k\right) / \left(\sum_{j=1}^{i-1} \rho_j + \rho_i\right) \tag{8}$$

and by dividing numerator and denominator by $\sum_{j=1}^{i-1} \rho_j$, we obtain:

$$H_i^k = \left(H_{i-1}^k + \delta_i C_i^k\right) / \left(1 + \delta_i\right) \tag{9}$$

where:

$$\delta_i = \rho_i / \sum_{j=1}^{i-1} \rho_j \tag{10}$$

~~We can finally write:~~ is the contribution of Area i relative to the contribution of all upstream Areas, i.e., what sediment is entering the river from Area i relative to what is already in the river. We will call δ_i the "relative contribution" from Area i

We can also write:

$$H_i^k - H_{i-1}^k = (C_i^k - H_i^k)\delta_i, \quad \text{for } i = 1, \cdots, M \text{ and } k = 1, \cdots, N \tag{11}$$

From this relationship we see that the relative changes in bin height between two successive sites along the main stream ~~tells us something~~ contain information about the present-day erosion rate in the intervening catchment, through the relative contributions δ_i and the relative concentrations in surface bedrock in Area i, C_i^k. If one knows either δ_i or the C_i^k (for $k = 1, \cdots, N$), one can derive the value of the other quantity(ies). For example Resentini and Malusà (2012) assumed that they knew the values of the C_i^k surface concentrations in each sub-catchment to derive estimates of the corresponding δ_i. Here we will try to assess whether the values of both the relative surface concentrations C_i^k and the relative contributions δ_i^k can be estimated.

2.4 Estimating erosion rates

Considering that we have M sites along the main river trunk and that we have selected to use N bins to describe the distributions of ages, we have $N \times M$ unknown values for the relative heights of the bins describing the distribution of ages in the source areas (the C_i^k) and another set of $M-1$ unknown values for the relative contributions δ_i. However, we only have $N \times M$ equations (see eq. 11) and the problem is clearly underdetermined, i.e. we have more unknowns than equations among the unknowns. This means that there is an infinite number of solutions that satisfy the equations. We cannot estimate the values of all unknowns, but, as we will show now, we can estimate bounds on the value of the unknowns δ_i. ~~However~~

Two cases must be considered. First, if there is a noticeable change in relative bin heights in the detrital record between sites $i-1$ and i, i.e. $H_i^k \neq H_{i-1}^k$, the distribution of ages in Area i, ~~if the relative bin heights do not change~~ C_i^k, must be

different from that in the river at site i, i.e. $C_i^k \neq H_i^k$ and, consequently, the relative contribution from Area i, δ_i must be finite, i.e. $\delta_i > 0$ and therefore $\epsilon_i > 0$. This means that there must be a minimum finite value for δ_i and therefore for ϵ_i to explain the difference in distribution between sites $i-1$ and i. We will call this minimum but finite value δ_i^m (and ϵ_i^m, respectively). There is another solution to consider where $\delta_i \to \infty$ and $C_i^k \to H_i^k$, which is correct regardless of the values of the H_{i-1}^k and which corresponds to the situation where the relative contribution from Area i is so large that it completely overprints the river signal. We thus have two bounds for the relative contributions δ_i at each site, one finite and the other infinite:

$$\delta_i \in [\delta_i^m, \infty] \tag{12}$$

The second case to consider is when the relative bin heights between two successive sites ~~(~~do not change , i.e. $H_i^k = H_{i-1}^k$ ~~),~~ ~~then~~ for all bins k. In this case, we cannot tell if this is because the erosion rate in catchment i is nil ($\epsilon_i = 0 \to \rho_i = 0 \to \delta_i = 0$), or because the signature of the source in catchment i, i.e. the distribution of ages at the surface, is identical to that of the ~~previous catchment~~ river ($C_i^k = H_i^k = H_{i-1}^k$), and we have no constraints on δ_i or the erosion rate in Area i. Although this situation may arise, we will now only consider the case where $H_i^k \neq H_{i-1}^k$ and try to find the value of δ_i^m.

2.5 ~~Inverting for C_i^k and ϵ_i~~

~~Using Equation (11), we can now obtain the unknown C_i^k recursively using:~~ For this, we re-write equation 11 as:

$$C_i^k = \frac{H_i^k - H_{i-1}^k}{\delta_i} + H_i^k \tag{13}$$

~~by making first the simplest assumption that $\epsilon_i = \epsilon_1$ for all i, which leads to:~~

$$\rho_i = \frac{A_i \alpha_i}{A_1 \alpha_1}$$

~~and~~

$$\delta_i = A_i \alpha_i / \sum_{j=1}^{i-1} A_j \alpha_j$$

~~Assuming a uniform erosion rate ($\epsilon_i = \epsilon_1$) should be regarded as~~Considering that the ~~zeroth-order scenario that should first be considered to explain the data; it may, however, lead to unrealistic solutions for any of the C_i^k,~~ H_i^k are relative bin heights, i.e. ~~values of C_i^k that are not in the range $[0,1]$. To avoid this we must add two conditions that affect the values for the unknown~~ $H_i^k \in [0,1]$ and $\sum_{k=1}^N H_i^k = 1$, implies that the C_i^k are also relative bin heights. Therefore we must have $\sum_{k=1}^N C_i^k = 1$ and $C_i^k \in [0,1]$. This leads to two constraints on the value of the relative contribution δ_i~~. $C_i^k > 0$ implies that:~~ :

$$C_i^k > 0 \to \delta_i > \max_{k=1,\cdots,N} \frac{H_{i-1}^k - H_i^k}{H_i^k} \text{ ~~for all~~ } k = 1, \cdots, N \tag{14}$$

and~~$C_i^k < 1$ implies, in turn, that:~~ :

$$\delta C_i \geq^k < 1 \to \delta_i > \max_{k=1,\cdots,N} \frac{H_i^k - H_{i-1}^k}{1 - H_i^k} \text{ ~~for all~~ } k = 1, \cdots, N \tag{15}$$

for all $i = 1, \cdots, M$. The first condition applies where there is a decrease in any relative bin height k between ~~locations~~ site $i-1$ and ~~location~~ site i, i.e. $H_i^k < H_{i-1}^k$, whereas the second condition applies where there is an increase in any relative bin height k between locations $i-1$ and i, i.e. $H_i^k > H_{i-1}^k$. We ~~make the further (and trivial) assumption that the true erosion rate must satisfy both conditions.~~ can therefore conclude that the minimum values of the contribution factors that are necessary to explain the change in relative bin size from site to site are given by:

$$\delta_i^m = \max_{k=1,\cdots,N} \left(\frac{H_{i-1}^k - H_i^k}{H_i^k}, \frac{H_i^k - H_{i-1}^k}{1 - H_i^k} \right) \quad \text{for } i = 1, \cdots, M \tag{16}$$

2.5 ~~Procedure summary for main trunk distributions~~

~~To obtain estimates of~~ From these estimates of the contribution factors, δ_i^m, we can then derive the value of the corresponding erosion rate in each ~~catchment, we then proceed sequentially for $i = 1, \cdots, M$, where M is the number of locations within the river where we have an age distribution. For each site~~ Area i, ~~we first compute δ_i according to:~~ ϵ_i^m, that is necessary to explain the observed variations in age distributions along the main river trunk, by using the following relationship that we derive in the appendix:

$$\delta\epsilon_i{}^m = \max_{k=1,\cdots,N} A \frac{F_1 \epsilon_1^m}{F_i} \delta_i \alpha_i / \sum{}^m \prod_{j=1}^{i-1} A(1 + \delta_j \alpha_j{}^m) \quad \text{for } i = 1, \frac{H_{i-1}^k - H_i^k}{H_i^k} \cdots, \frac{H_i^k - H_{i-1}^k}{1 - H_i^k} M \tag{17}$$

~~From this value of δ_i, we can deduce an erosion rate (relative to the~~ assuming that $\delta_1^m = 0$ and $\epsilon_1^m = 1$ such that the estimated minimum erosion rates are relative erosion rates scaled by the unknown erosion rate in the first catchment~~, ϵ_1) from:~~

$$\epsilon_i = \frac{\delta_i}{A_i \alpha_i} \sum_{j=1}^{i-1} A_j \alpha_j \epsilon_j$$

~~as well as the relative concentration of grains of age in~~ .

From the values of the minimum contribution factors, δ_i^m, we can also estimate the relative surface concentrations of each age bin k in ~~Area A_i~~ each catchment i, using:

$$C_i^k = \frac{H_i^k - H_{i-1}^k}{\delta_i} \frac{H_i^k - H_{i-1}^k}{\delta_i^m} + H_i^k \tag{18}$$

~~for all $k = 1, \cdots, N$. For the first catchment, i.e. $i = 1$, we assume that $\epsilon_1 = 1$ and $C_i^k = H_i^k$.~~

3 Using age distributions from tributaries

Age distributions from tributaries can be included to improve the solution locally, i.e. in the ~~catchment that includes the tributary~~ tributary catchment. Let's call A_T, α_t and ϵ_T the catchment area, the ~~abundance of the target mineral in surface rocks~~ mineral concentration factor and the mean erosion rate of the ~~catchment of the tributary~~ tributary catchment, and A_M, α_M and ϵ_M the

catchment area, the ~~abundance of the target mineral in surface rocks~~ mineral concentration factor and the mean erosion rate of the rest of catchment ~~A_i~~ i.

For each bin k in the catchment i, we can write:

$$A F_i \epsilon_i \alpha_i {}^m_\sim C_i^k = A F_T \epsilon_T \alpha_T C_T^k + A F_M \epsilon_M \alpha_M C_M^k \tag{19}$$

where $F_T = A_T \alpha_T$ and $F_M = A_M \alpha_M$. By conservation of eroded rock mass, we have:

$$A F_M \epsilon_M \alpha_M = A F_i \epsilon_i \alpha_i - A^m - F_T \epsilon_T \alpha_T \tag{20}$$

which we can use to transform Equation (19) into:

$$A F_i \epsilon_i \alpha_i {}^m_\sim C_i^k = A F_T \epsilon_T \alpha_T C_T^k + (A F_i \epsilon_i \alpha_i - A^m - F_T \epsilon_T \alpha_T) C_M^k \tag{21}$$

to obtain:

$$C_M^k = \frac{A_i \epsilon_i \alpha_i C_i^k - A_T \epsilon_T \alpha_T C_T^k}{A_i \epsilon_i \alpha_i - A_T \epsilon_T \alpha_T} \frac{F_i \epsilon_i^m C_i^k - F_T \epsilon_T C_T^k}{F_i \epsilon_i^m - F_T \epsilon_T} \tag{22}$$

Using the method for the main trunk data described in the previous sections, we know ϵ_i and C_i^k. The tributary data (age distributions) gives us the C_T^k ~~(~~surface concentrations as measured in the tributary stream (i.e. $C_T^k = H_T^k$ ~~because ...~~) and we can solve for the surface concentrations C_M^k assuming first that the erosion rate is uniform in the catchment i, i.e. $\epsilon_T = \epsilon_M = \epsilon_i$, to give:

$$C_M^k = \frac{A_i \alpha_i C_i^k - A_T \alpha_T C_T^k}{A_i \alpha_i - A_T \alpha_T} \frac{F_i C_i^k - F_T C_T^k}{F_i - F_T} \tag{23}$$

However, this may lead to unrealistic values of the relative surface concentrations C_M^k, i.e. not comprised between 0 and 1. Consequently, two conditions need to be added so that $0 < C_M^k < 1$ for all k ~~which might yield to erosion rate estimate in the tributary catchment, ϵ_T, different from ϵ_i obtained for A_i~~. The first condition ($C_M^k > 0$) yields:

$$\epsilon_T < \frac{A_i \alpha_i C_i^k}{A_T \alpha_T C_T^k} \frac{F_i C_i^k}{F_T C_T^k} \epsilon_i {}^m_\sim \tag{24}$$

while the second condition ($C_M^k < 1$) yields:

$$\epsilon_T < \frac{A_i \alpha_i (1 - C_i^k)}{A_T \alpha_T (1 - C_T^k)} \frac{F_i (1 - C_i^k)}{F_T (1 - C_T^k)} \epsilon_i {}^m_\sim \tag{25}$$

The true erosion rate must satisfy both conditions and we therefore select the smallest value of ϵ_T obtained by considering any relative surface concentration difference between the tributary sub-catchment concentration (C_T^k) and that of the entire catchment (C_i^k).

3.1 ~~Procedure summary for tributary distributions~~Uncertainty estimates by bootstrapping

~~In summary, we first compute the erosion rate in the sub-catchment of the tributary, according to:~~

$$\epsilon_T = \min_{k=1,\cdots,N} \left(\epsilon_i, \frac{A_i \alpha_i C_i^k}{A_T \alpha_T C_T^k} \epsilon_i, \frac{A_i \alpha_i (1 - C_i^k)}{A_T \alpha_T (1 - C_T^k)} \epsilon_i \right)$$

~~and we then use it to compute the C_M^k according to:~~

$$C_M^k = \frac{A_i \epsilon_i \alpha_i C_i^k - A_T \epsilon_T \alpha_T C_T^k}{A_i \epsilon_i \alpha_i - A_T \epsilon_T \alpha_T}$$

~~from the values of C_i^k and ϵ_i obtained from the trunk data analysis and the C_T^k obtained form the measured distribution in the tributary.~~

~~If there are more than one tributary in a catchment, we repeat the operation for each tributary, using the previously computed ϵ_i and C_i^k from the main trunk analysis, under the assumption that the tributaries have disconnected drainage areas in the catchment i.~~

4 ~~Uncertainty estimates by bootstrapping~~

We assess the ~~uncertainty~~ robustness of our estimates of ~~erosion rate ϵ_i and~~ minimum erosion rate ϵ_i^m and corresponding relative concentrations C_i^k, derived from finite size samples by bootstrapping. For this, we simply use the method described above on a large number of sub-samples of the observed distributions constructed by ~~arbitrarily and randomly removing 25%~~ random sampling of the observed ~~age estimates~~distributions with replacement. This yields distributions of erosion rate and relative concentrations that can be used to estimate the uncertainty arising from the finite sample size. These distributions are usually not normal and we use their ~~modal~~ median value, rather than their mean, as the most likely estimate of erosion rate and their standard deviation to represent uncertainty.

The code is provided as a Jupyter Notebook containing ~~R-code~~ python code and explanatory notes that refer to the equations given in this manuscript. The user must provide a series of input files containing (a) the description of the sites, i.e. the order in which the sites are located along the river, whether they drain into the main river stem or into a tributary, the drainage area A, the ~~lithological~~ mineral concentration factor α, (b) the bin sizes and (c) the observed age data at each site. The code produces distributions of estimates of erosion rate and relative concentration of grains of ages within each ~~range, their mean value, standard deviation and modal values (~~bin for each site from the bootstrapping~~)~~.

4 ~~Applications to detrital age~~ Assessing the method on synthetic distributions

~~To illustrate the method~~We have assessed the reliability of the erosion rate estimates obtained from the method by applying it to synthetic age distributions made of $N = 4$ age bins at $M = 5$ sites. We have assumed known mineral concentration factors, α_i, contributing areas, A_i, and relative erosion rates. To construct the distributions, we created very large samples (10^6 grains)

from normal distributions of grains having ages centered on 4 peak values (20, ~~we now apply it to a detrital age datasets from the Eastern Himalaya. The ages correspond to cooling ages,~~ 40, 60 and 80 Myr) with a standard deviation of $\Delta a = 5$ Myr. The amplitude of the peaks is first set to $(0,0,0,1)$, $(0,0,1,0)$, $(0,1,0,0)$, $(1,0,0,0)$ and $(0,0,0.5,0.5)$, for the five sites. In this way, we are likely to maximize relative bin height differences between two consecutive sites. We will later relax this assumption and see how it impacts the estimates obtained by the method. We then constructed 5 grain distributions corresponding to each of the sites by adding the original distributions in proportions given by the relative contributions (product of area, mineral concentration factor and erosion rate) of each area. We then sampled these distributions by randomly selecting $n = 100$ grains. This number was chosen because, in many detrital age studies, it represents the average number of grains collected at any given site. We applied our method to these synthetic datasets to obtain distributions of minimum erosion rate by bootstrapping and took the median value as a reliable estimate of the minimum erosion rate in each area necessary to satisfy the synthetic age distributions. We repeated this operation 1000 times (i.e. ~~-~~by generating 1000 synthetic datasets) to obtain the distributions of estimates of minimum erosion rates and compared them to the imposed erosion rates used to construct the synthetic age distributions. In a first set of four experiments, the areas and mineral concentration factors are identical for each site. In the first experiment, the erosion rates are chosen to vary greatly (by up to two orders of magnitude) between consecutive sites. In the second experiment, all sites have the same erosion rate, in the third experiment, the erosion rate increases by a factor two from site to site and in the fourth experiment, the erosion rate decreases by a factor two from site to site. The results are shown in Figure (3).

We see that the estimated erosion rates (median value) are in good agreement with the imposed (true) erosion rates, especially when large jumps in erosion rate exists between successive sites/catchments. However, in some cases, there appears to be an artificial increase in estimated erosion rate from site to site. This is clearly seen in the case where the imposed erosion rate is assumed uniform at all sites or to decrease from site to site. In both cases, the method predicts an apparent (or spurious) increase in erosion rate at the last site.

To determine what controls the reliability of these estimates, we performed two other sets of experiments. The first assumes random amplitudes for the peaks in each of the catchment (Figure 4) and the seconds assumes that the ~~time in the past when the rocks cooled through a given closure temperature. The datasets that we use contain ages that were~~ F_i (product of drainage area A_i by relative abundance α_i) increase downstream (Figure 5). When the amplitudes of the peaks are random, the differences in peak height between two successive sites is much smaller, leading to deteriorated values for the estimated erosion rates. Oppositely, when the contributing areas (or relative abundances) increase downstream, the estimates are improved.

Consequently, the accuracy of the estimates of erosion rate obtained from our method rely on whether the two successive age distributions used to estimate the δ_i^m are markedly different and whether the size of the two successive catchments increases or, at least, does not decrease substantially. These conditions should be kept in mind when interpreting the results obtained by our method.

5 Applications to a detrital age dataset

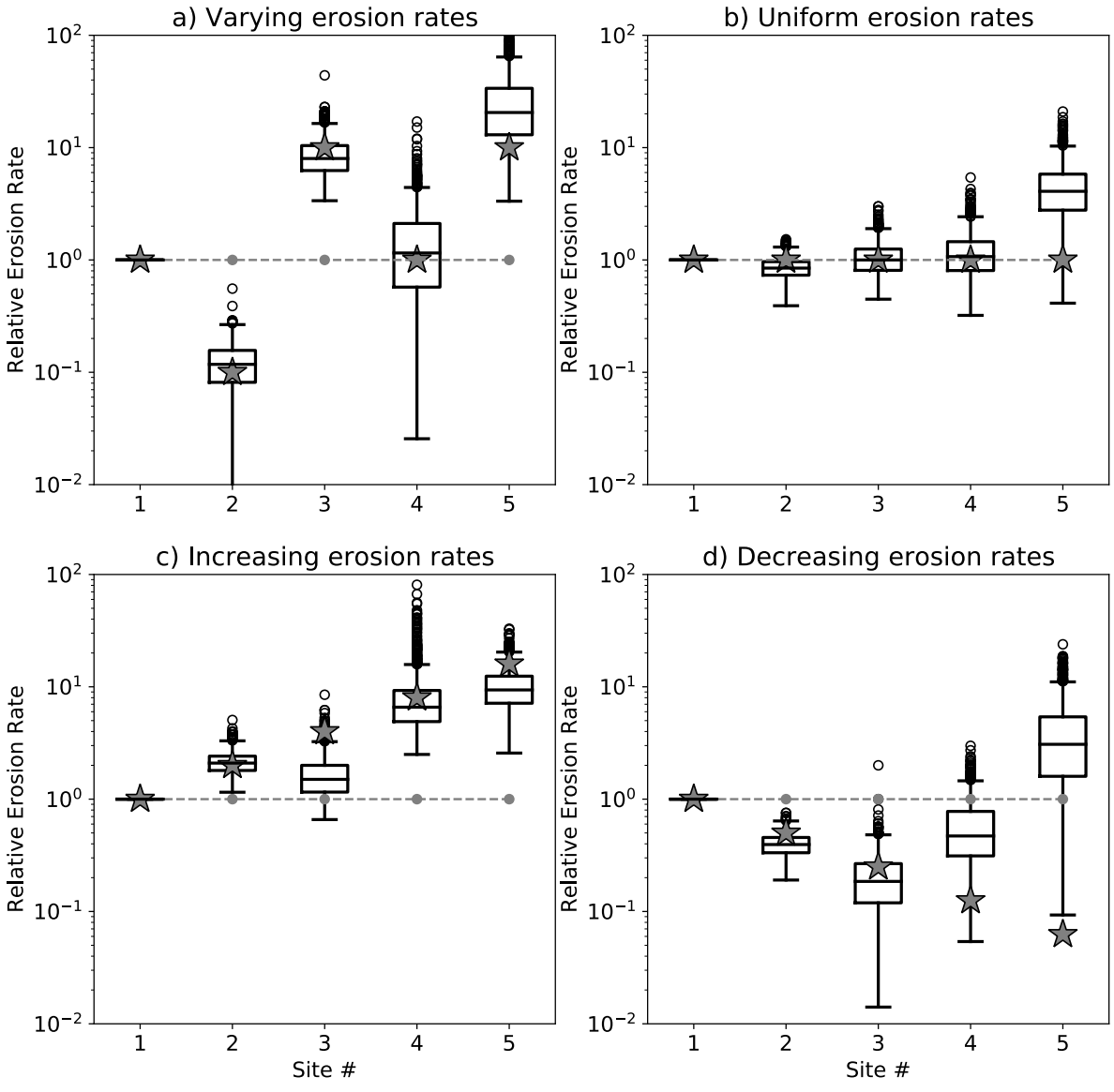

Figure 3. Results of the method applied to the first set of synthetic datasets. Computed erosion rate distributions for four synthetic datasets. For each distribution, the box extends from the lower to upper quartile values, the line corresponds to the median value and whiskers extend from the box to show the range of the erosion rate estimates, excluding outliers. Outliers are indicated by small circles past the end of the whiskers. For each site, the grey stars correspond to the imposed erosion rates and the dashed grey line gives the product of the imposed area and fertility factors, $F_i = A_i \alpha_i$.

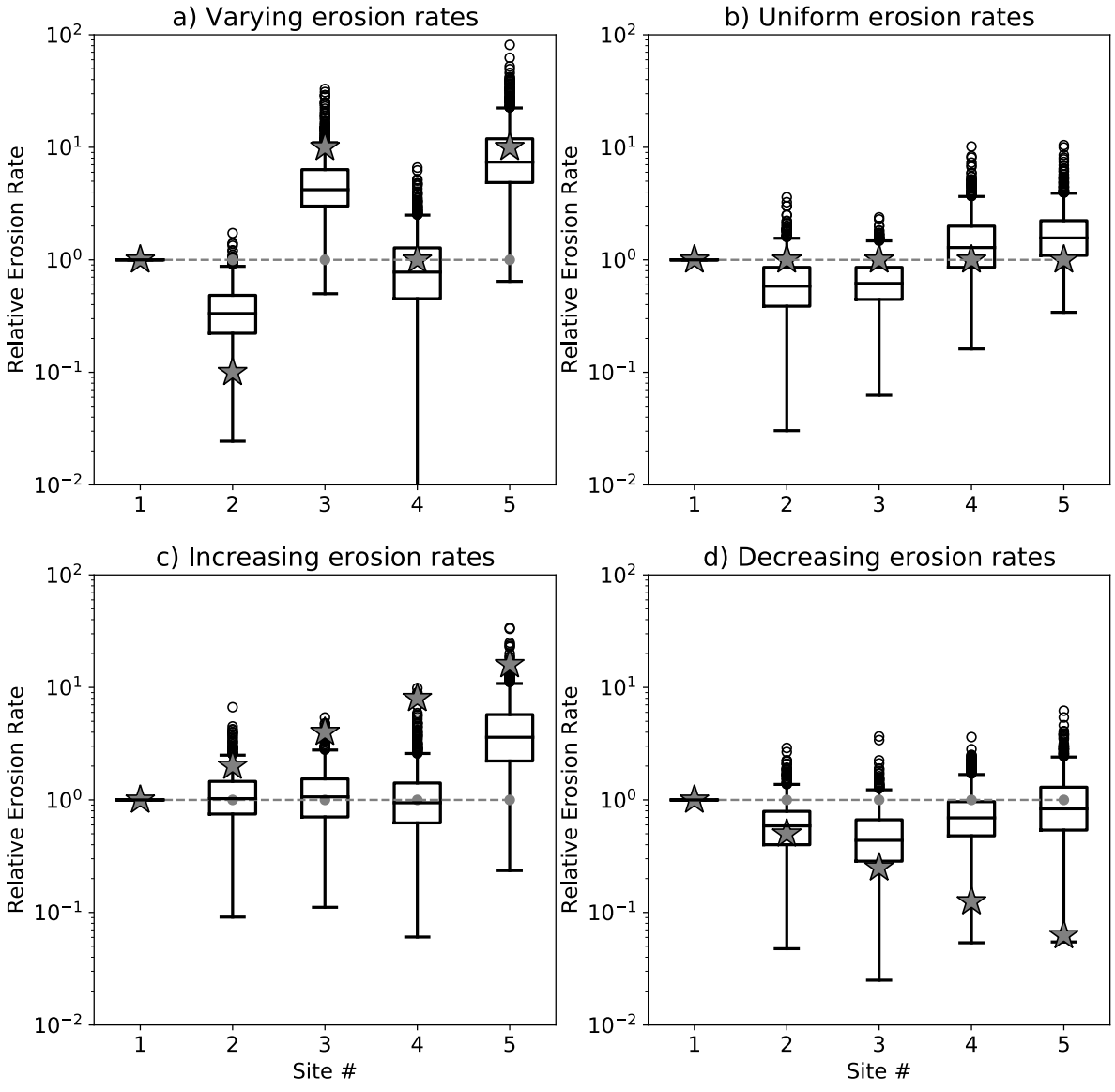

Figure 4. Results of the method applied to the second set of synthetic datasets with random peak amplitudes. See Figure 3 caption for further details.

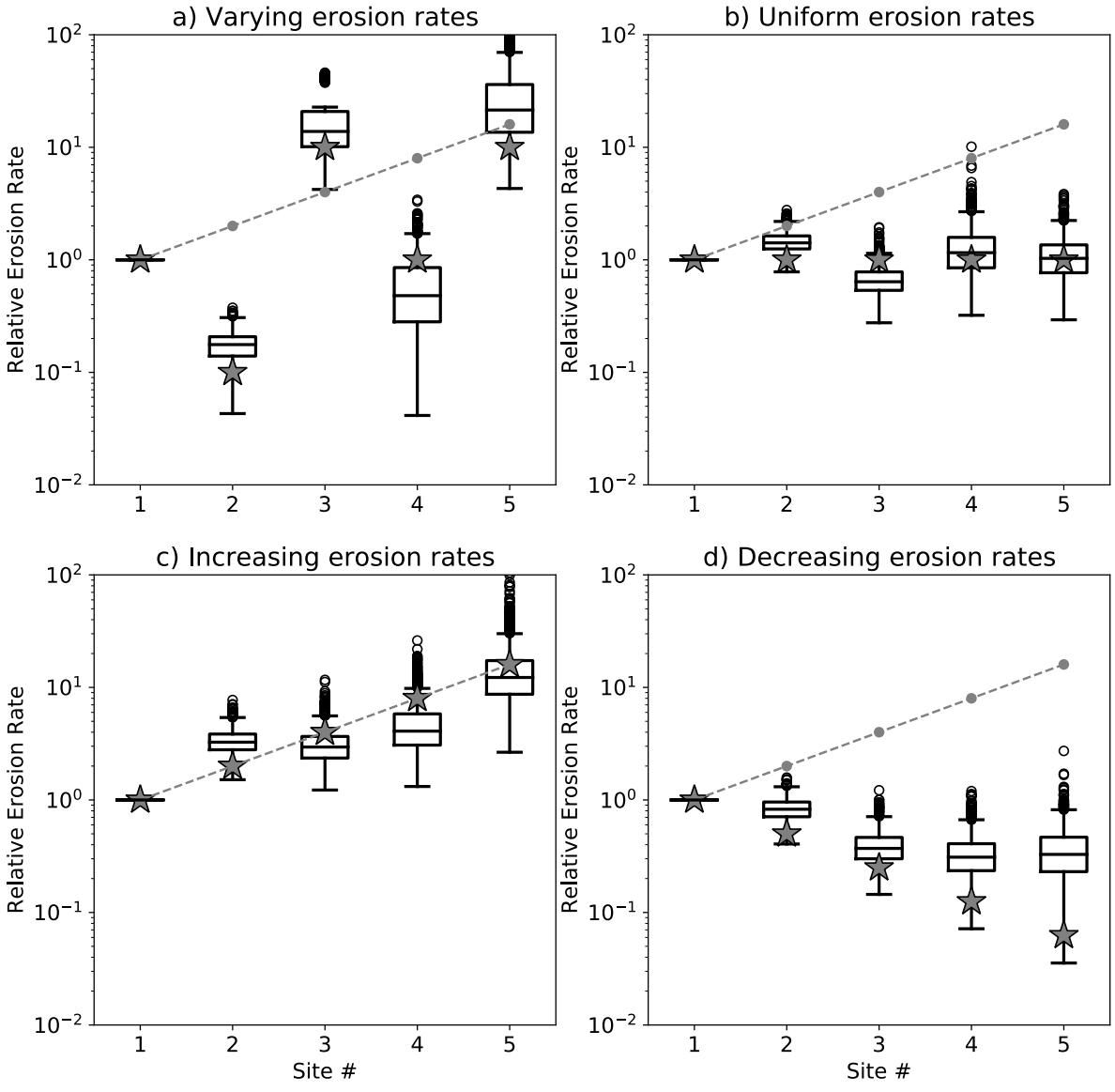

Figure 5. Results of the method applied to the second set of synthetic datasets with increasing $F_i = A_i \alpha_i$ downstream. See Figure 3 caption for further details.

Table 1. Age bins used to construct age distributions shown in Figure ~~??~~ 8 and used in our example.

Bin 1	Bin2	Bin 3	Bin 4	Bin 5
0-5 Ma	5-10 Ma	10-20 Ma	20-50 Ma	50-500 Ma

To illustrate the method, we now apply it to a detrital age dataset from the Eastern Himalaya that contains ages obtained using the muscovite $^{40}Ar/^{39}Ar$ thermochronometer~~, which has a closure temperature $T_c \approx 385 \pm 70°C$ (Hames and Bowring, 1994), depending on grain size, chemistry, and cooling rate.~~

~~Age distributions were constructed~~ . The data were combined from published age datasets collected along the main trunk of the Tsangpo-Siang-Brahmaputra river system, as well as along some of its tributaries (Figure 6), using age bins given in Table 1. Samples A,B,C (composite sample), X and Y are from Lang et al. (2016) and samples Z, T-40a and T-41a are from Bracciali et al. (2016). The complete age datasets are given in the Data Repository, Table S1. In Table 2, we give the relative position of the successive samples along the main trunk of the river, i, the respective exclusive contributing areas, A_i and the ~~lithological factor~~mineral concentration factors, α_i~~, (or abundances of~~ . We first used constant values of 1% (fourth column in Table 2). We will also use variable values for the mineral concentration factors, making the simple assumption that surficial rocks have an average mineral composition that depends mostly on their lithology. A very simple way to proceed is to look at the surface lithology indicated in the geological map of the region for each studied catchment. In this case we used the geologic map of the Eastern Himalaya from Yin et al. (2010). The semi-quantitative α-values computed for each catchments are given in the fifth column of Table 2. We are aware that, for such a complex and vast area, this approximation can yield to poor estimates of the concentration of the target mineral in surface rocks~~)~~. For more accurate methods (that also require additional data), we refer the user to published work by others that have investigated this issue by looking, for instance, at petrographic and heavy mineral density in modern river sediments such as SRD index (Garzanti and Andò, 2007) or the method proposed to compute mineral "fertility" (Malusà et al., 2016).

We will investigate the effect of using variable concentrations of muscovite-bearing rocks in each of the catchments as derived from a geological map of the area (fifth column in Table 2).

~~Observed distributions of ages (light grey bars) in samples collected at sites shown in Figure 6 and predicted surface age distributions (dark grey bars) in corresponding catchment areas. Data and results are shown for the sites along the main trunk only.~~

~~Computed relative erosion rates, variance and modal values obtained from the mixing model and the bootstrapping procedure. Values are normalized such that the mean is 1. Site names refer to locations shown in Figure 6. Site Mean erosion rate St. deviation Modal value(mm/yr) (mm/yr) (mm/yr)TG-40a 0.012 0.000 0.012 TG-41a 0.017 0.011 0.012 A 0.059 0.031 0.040 Y 0.92 0.56 0.60 B 0.92 0.56 0.60 X 0.48 0.27 0.31 C 4.5 2.9 2.8 Z 0.48 0.27 0.31~~

Results are shown in ~~Table 7 as computed relative~~ Figure (7) as distributions of computed relative minimum erosion rates (i.e. normalized such that the mean erosion rate is 1) ~~, standard deviations and modal values~~obtained by bootstrapping. The computed surface concentrations, C_i^k, for each site i are shown in Figure (8). Figure ~~9~~ (9) contains maps of the various

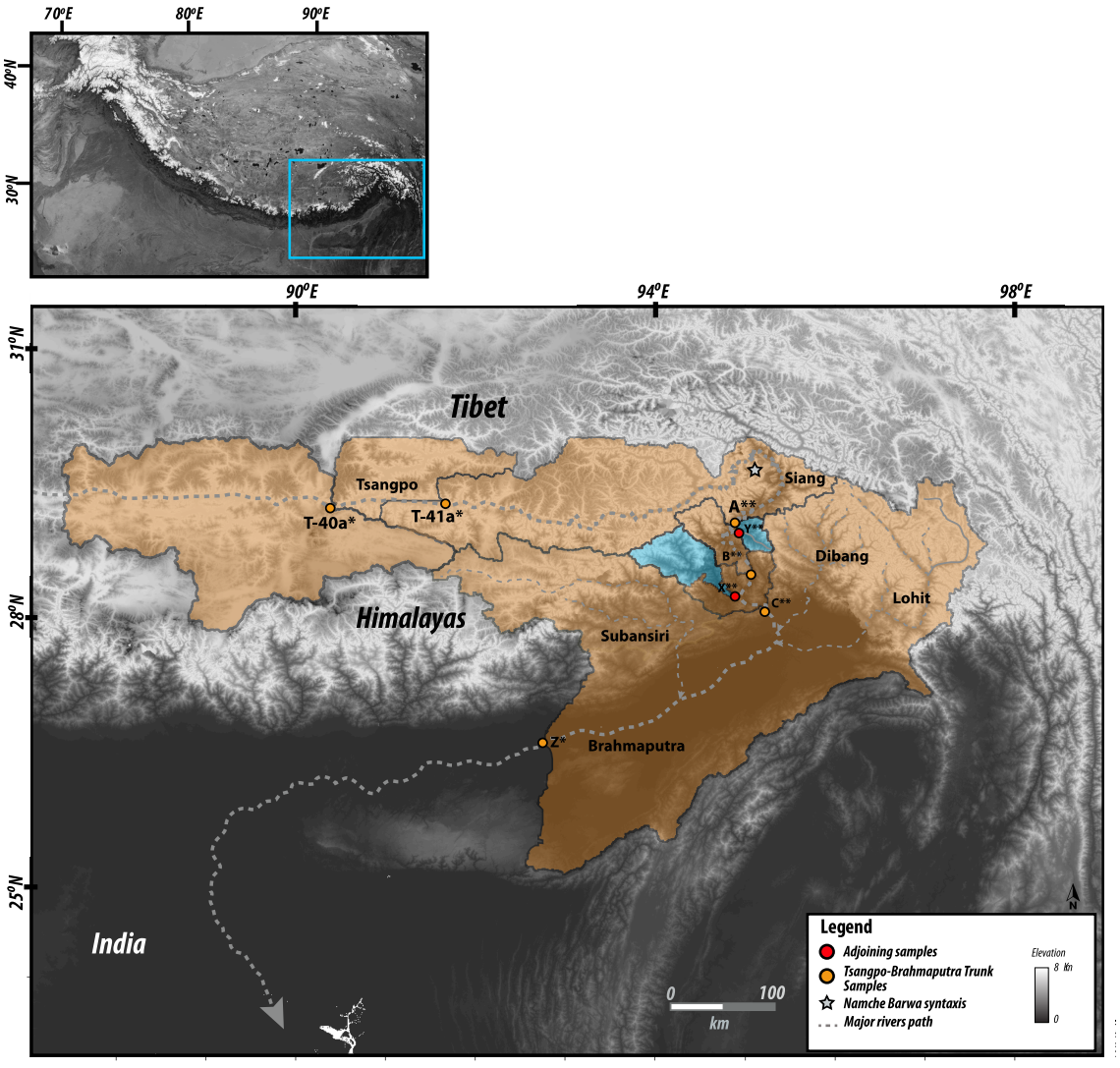

Figure 6. a) Location of the study area and b) location and name of sampling sites and geometry of the drainage basins contributing to each site.The orange shading represents catchments draining directly into the main trunk; pale blue shading represents the tributary catchments or sub-catchments.

Table 2. Relative position along the main trunk of the Tsangpo-Siang-Brahmaputra river system. Negative numbers indicate samples collected along a tributary. Catchment areas and ~~lithological~~ mineral concentration factors used to compute the erosion rate reported in Table 7. The two columns correspond to two different sets of values used for comparison. Site names refer to locations shown in Figure 6.

Site	Position	Catchment area (km^2)	~~Lithological factor~~ mineral concentration factor 1	mineral concentration factor 2	Refere
TG-40a	1	55395	0.01	0.03	Bracciali et al. (20
TG-41a	2	13265	0.01	0.03	Bracciali et al. (20
A	3	41374	~~0.0135~~ 0.01	0.02	Lang et al. (20
Y	-4	1250	~~0.013~~ 0.01	0.25	Lang et al. (20
B	5	2092	~~0.013~~ 0.01	0.09	Lang et al. (20
X	-6	2135	~~0.011~~ 0.01	0.18	Lang et al. (20
C	7	1451	~~0.0123~~ 0.01	0.12	Lang et al. (20
Z	8	111706	~~0.0131~~ 0.01	0.30	Bracciali et al. (20

catchments shaded according to their predicted ~~modal~~ median erosion rate and surface concentrations of grains of age within each range~~, obtained from the bootstrapping and mixing algorithms described above~~. Predicted concentrations are scaled such that the sum of the five age bin concentrations is 1 in each catchment. We see that predicted minimum erosion rates increase by about two orders of magnitude with distance along the main river trunk from its source area along the southern margin of the Tibetan Plateau. Maximum erosion rates are observed in catchment C (and sub-catchment X) that is closest to the eastern Himalayan ~~syntax.~~ syntaxis. The amplitude of the jumps in erosion rate between sites A and B, and B and C are potentially amplified by our method because sites A, B and C have relatively small areas, A_i and contains relatively uniform distributions of ages among the five bins. As we have noticed in our synthetic examples, this may lead to a spurious increase in erosion rate. Further downstream (catchment Z), the predicted minimum erosion rate remains high but lower than observed near the ~~syntax.~~ syntaxis. This estimate is likely to be robust as site Z has a very large contributing area and has an age distribution that is markedly different from that of the previous catchment (C).

The most salient result predicted by the method is that the erosion rate in the easter Himalayan syntaxis should be at least 5-7 times higher than the mean erosion rate along the Tsangpo-Siang-Brahmaputra basin. This estimate is in good agreement with the conclusions of Stewart et al. (2008) who used U-Pb ages of detrital zircon grains from the Brahmaputra River to demonstrate that approximately half of the sediment flux carried by the Brahmaputra River originates from an area around the eastern syntaxis that represents only 2% of the total area of the river drainage basin. This implies that erosion rate in the vicinity of the syntaxis should be approximately 25 times higher than the mean erosion rate. Similar estimates were obtained by Enkelmann et al. (2011) using a larger detrital age dataset from the area, while a relatively smaller estimate (erosion rate should only be 5 times higher than the mean in the syntaxis area) was obtained by Singh and France-Lanord (2002) using the isotopic composition of sediments collected along the Brahmaputra River. In Table 3, we compare the erosion rate estimates obtained using uniform surface concentration factors ($\alpha_i = 0.01$) with those obtained using variables values (given in the fifth

Table 3. Predicted erosion rate in the successive sub-catchments obtained by assuming uniform values for the α_i and variable values derived from the relative abundance of muscovite-bearing surface rock in the geological map.

Site	Erosion rate estimate using uniform α_i	Erosion rate estimate using variable α_i
TG-40a	1	1
TG-41a	1.06	1.12
A	0.78	1.17
Y	5.29	1.54
B	5.39	1.98
X	36.4	8.71
C	36.4	8.77
Z	9.40	0.90

column of Table 2). We note that although the values obtained for the sub-catchments upstream of the syntaxis (sites Y and B) are somewhat reduced, the very large relative erosion rates (5-8 times the entire basin average) predicted in the syntaxis (sites X and C) is a robust outcome of the method.

We also note that erosion rates in sub-catchments Y and X do not need to be noticeably smaller than the estimates of erosion rate in their host catchments (B and C). As explained earlier, the true erosion rates could be larger than those of their host catchments. This could be the case for sub-catchment Y where we predict an erosion rate identical to that of catchment B. These estimates are likely to be reliable because their area is similar to that of their sub-catchment (they occupy a non-negligible portion of their host catchment) and because they have strikingly different age distributions than their host catchments (B and C) (Figure 8). One can also see from the age distributions shown in Figure (8) how the large contribution from bin 4 at site Y affects the relative height of bin 4 at site B and, similarly, how the large contribution from bin 3 affects the relative height of bin 3 at site C.

Interestingly, there is a good correspondence between present-day erosion rate and where the youngest ages are being generated (~~compare upper left panel showing relative concentration of youngest age bin, to central panel showing predicted present-day erosion rate~~sites B and C), with the notable exception of the most downstream catchment (Z). In other words, where the mixing analysis predicts high minimum erosion rate to account for a substantial change in the age distribution between two adjacent catchments, is also where it predicts the highest concentration of young ages in the surface rocks. At the downstream end of the river (Catchment Z), we predict a relatively high minimum erosion rate from the mixing model but a relatively low concentration of young ages in comparison to the other catchments. This could mean that, in catchment Z, the present-day high erosion rate is relatively recent and has not led yet to a complete resetting of cooling ages which were set during earlier events.

We also note ~~(Table~~that the difference between the two quartile values (vertical size of the boxes in Figure 7 and ~~Figure ??)~~ ~~that all erosion rate distributions predicted by the bootstrapping method are highly asymmetrical, as the median value is~~

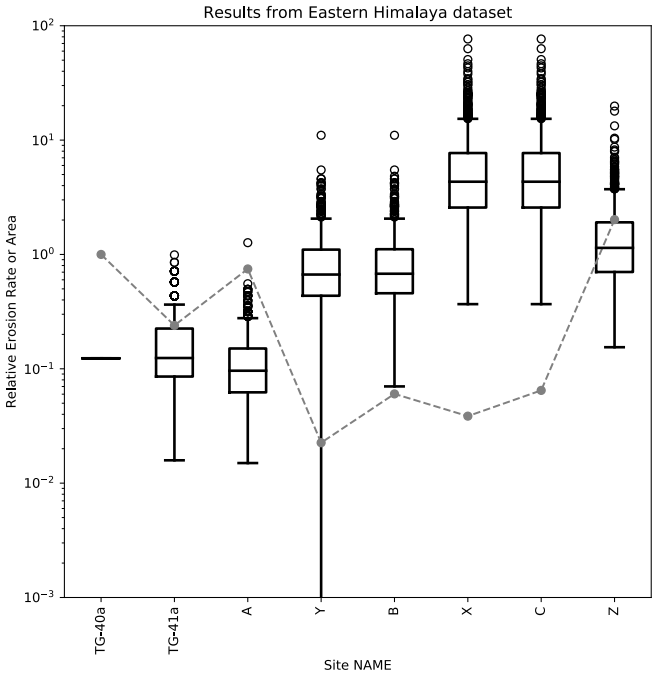

Figure 7. Computed erosion rate distributions obtained by applying the method to a Himalayan dataset. For each distribution, the box extends from the lower to upper quartile values, the line corresponds to the median value and whiskers extend from the box to show the range of the erosion rate estimates, excluding outliers. Outliers are indicated by small circles past the end of the whiskers. Erosion rate values are normalized such that the mean is 1. The grey circles connected by a dashed grey line are the product of the imposed area and mineral concentration factors, $F_i = A_i \alpha_i$ at each site. Site names refer to locations shown in Figure 6.

~~always significantly smaller than the mean. The standard deviation is~~ 8) is large, of the order of ~~30-50% of the mean value or~~ 50-100% of the ~~modal~~ median value of predicted erosion rate values. This indicates that our method can only provide order-of-magnitude estimates of the minimum erosion rate necessary to explain the age distributions. Interestingly, the ~~standard deviation~~ difference between the two quartile values does not increase downstream, which demonstrates that the uncertainty introduced by using incomplete or non-representative sub-samples of the true distributions at each of the station does not accumulate as our algorithm proceeds from station to station. This results from the incremental nature of our algorithm, as shown by Equation 11.

~~Distributions of predicted present-day erosion rate in mm/yr as derived by bootstrapping. See Figure (**??**) for sites locations.~~

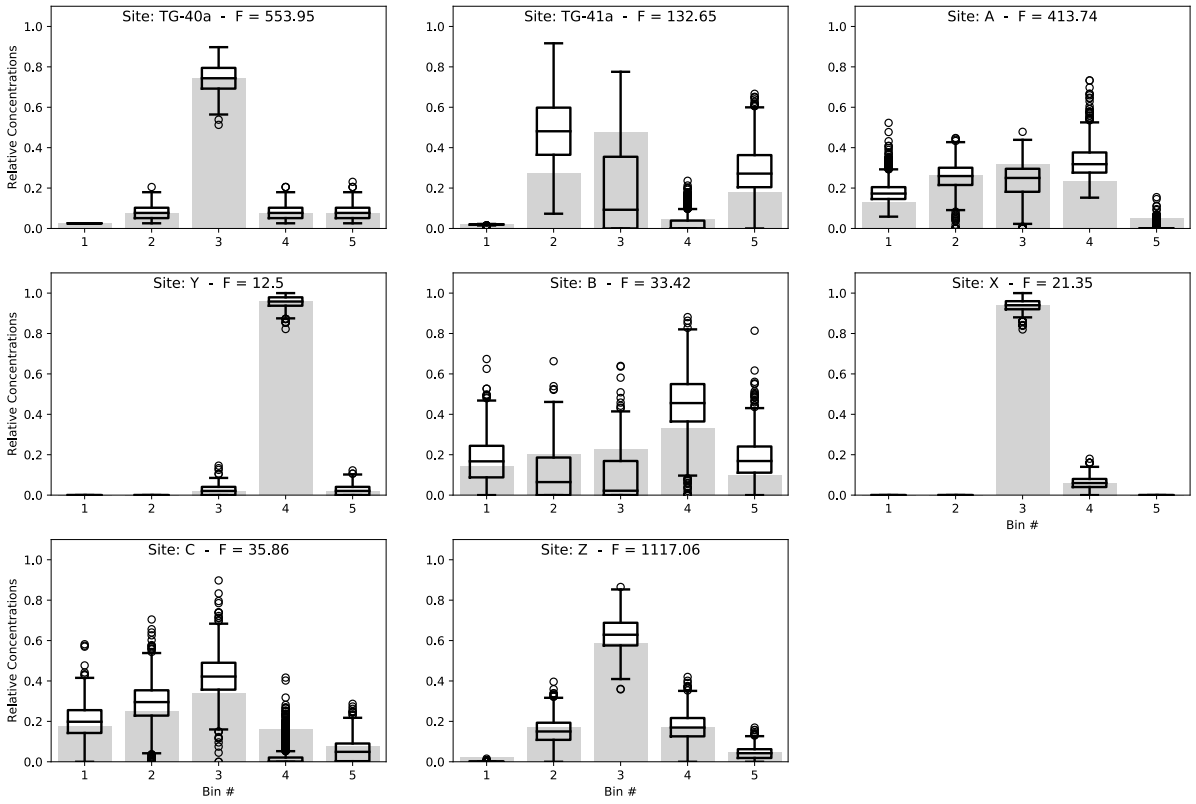

Figure 8. ~~Predicted modal erosion rates~~ Observed distributions of ages (~~central panel~~light grey bars) ~~and relative~~ in samples collected at sites shown in Figure 6 on which the distributions of predicted surface age ~~concentration~~ distributions have been superimposed for each site. For each distribution, the box extends from the ~~Muscovite detrital data~~ lower to upper quartile values, the line corresponds to the median value and whiskers extend from ~~Eastern Himalaya~~the box to show the full range, excluding outliers. ~~See Figure (??) for data distribution~~Outliers are indicated by small circles past the end of the whiskers.

6 Mineral concentration factors and their uncertainty

One of the ~~main source of error/~~sources of uncertainty in our estimates of the erosion rate comes from the assumed value of the ~~lithological~~ mineral concentration factors, α_i, which might be difficult to estimate in many situations (Malusà et al., 2016). We can compute the uncertainty on the erosion rates, $\Delta\epsilon_i$ arising from the uncertainty on the ~~lithological~~ mineral concentration factors, $\Delta\alpha_i$, from:

$$\Delta\epsilon_i = \sqrt{\sum_{k=1}^{i} \left(\frac{\partial\epsilon_i}{\partial\alpha_k}\right)^2 \Delta\alpha_k^2} \tag{26}$$

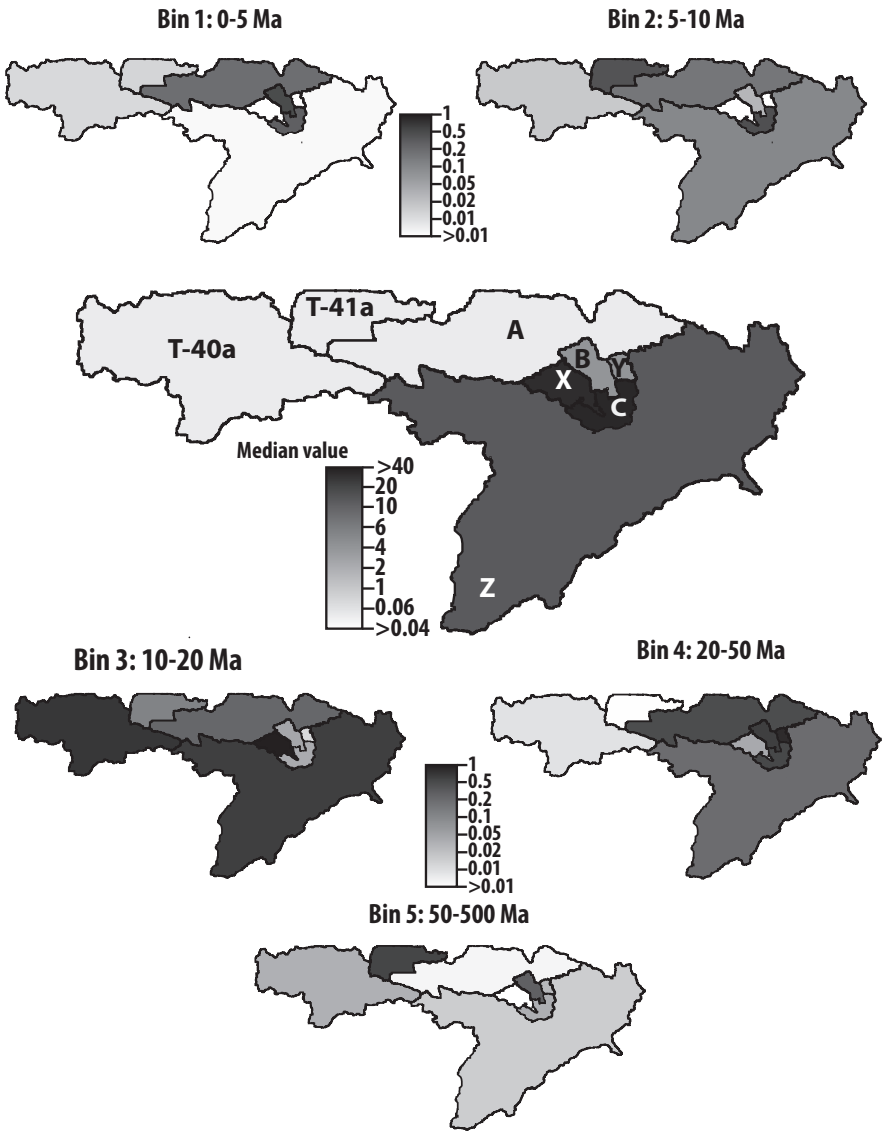

Figure 9. Maps of predicted median erosion rates (central panel) and relative surface age concentrations from the Muscovite detrital data from Eastern Himalaya. See Figures (8) and (8) for full distributions and data.

where:

$$\frac{\partial \epsilon_i}{\partial \alpha_k} = \left\{ \begin{array}{ll} 0 & \text{if } k > i \\ \frac{\epsilon_i}{\alpha_i} & \text{if } k = i \\ \frac{\delta_i^m}{F_i}\left(A_k \epsilon_k + \sum_{j=1}^{i-1} F_j \frac{\partial \epsilon_j}{\partial \alpha_k}\right) & \text{if } k < i \end{array} \right\} \quad (27)$$

The results are shown in Figure 10 as a plot of the ratio between the relative uncertainty in estimates of erosion rate $\Delta\epsilon_i/\epsilon_i$ and the relative uncertainty in ~~lithological~~ mineral concentration factors, $\Delta\alpha_i/\alpha_i$, for the six stations located along the main river trunk. We see that the relative uncertainty in erosion rate is approximately proportional to the relative uncertainty in ~~lithological~~ mineral concentration factor (i.e. all values are close to 1) and that there is only a minor downstream propagation of the uncertainty . This is also a simple consequence of the incremental nature of our algorithm, as explained by Equation 11.

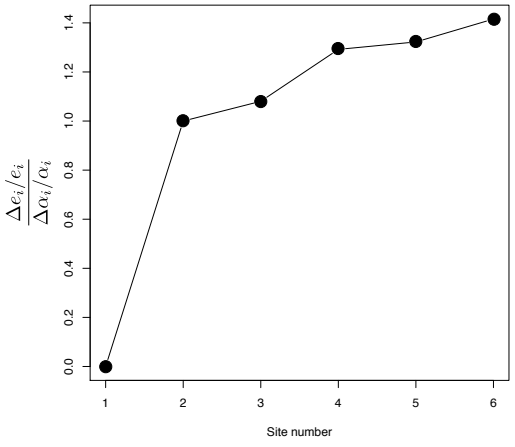

Figure 10. Relative uncertainty in erosion rate scaled by the relative uncertainty in ~~lithological~~ mineral concentration factor for the estimates obtained at each of the six sites along the main river trunk. The first site has a fixed relative erosion rate (=1) and therefore no uncertainty.

7 Ways in which the method could be improved

As described in this paper, our methods relies on the existence of age clusters (or bins) that can be found in the age distributions collected at various sites along a river. The method could be generalized by constructing kernel density estimates of the distribution of ages at each sites. These could be used to estimate the minimum contribution factors, δ_i^m, by applying condition (16) for the complete range of ages, not just the discrete values obtained by binning. We have found, however, that the solution we obtain in this way is strongly dependent on the choice made for the kernel and further investigation of this issue is required. Alternatively, estimates of cumulative density functions could be built directly from the data and, in turn, used to impose

condition (16) and estimate the minimum contribution factors, δ_i^m. However the limited number of grains at each site makes the comparison between two successive CDFs rather inaccurate. The accuracy of this approach can be tested by increasing the number of bins in our model such that N becomes similar to the average number of grains in any dataset. This leads to an overestimation of the minimum contribution factors. Clearly more work is required to investigate better or alternative ways to compare two successive age distributions.

8 Conclusions

We have developed a simple method to extract spatially variable erosion rates and surface age distributions from detrital ~~cooling age~~ cooling-age datasets from modern river sands. The method is based on what we believe are the simplest assumptions necessary to interpret such data and does not rely on a-priori knowledge of the distribution of ages in surrounding catchments. In describing the method we ~~demonstrate~~ have demonstrated that it is ~~well~~ suited to extract ~~from detrital cooling age datasets two seemingly independent~~ two seemingly sources of information pertaining to the spatial distribution of ~~present-day~~ erosion rate along the river. The first comes from using the age distributions as fingerprints characterizing the areas between two successive sites where detrital samples were collected. This allows us to predict first-order estimates of the relative erosion rate between these areas and the distribution of ages in surficial rocks in each area. These estimates of age distributions can be used as a second independent information on the past and present erosion rate in each area.

By applying the method to an existing dataset from the eastern Himalaya, we show that the method provides estimates of present-day erosion rate patterns in the area ~~,~~ that is consistent with previous, independent estimates, potentially evidencing that the fast present-day erosion rates in some parts of the study area are relatively young. We stress, however, that our method can only provide reliable estimates of erosion rate when the age distributions observed at two successive sites are different.

Importantly, the method is limited to providing the spatial distribution of erosion rate; independent information is necessary to transform those into absolute estimates of erosion rate.

9 Appendix

From the definition of the relative contributions, δ_i:

$$\delta_i = \frac{\rho_i}{\sum_{j=1}^{i-1} \rho_j} \quad \text{for } i = 2, \cdots, M \tag{28}$$

where:

$$\rho_i = \frac{F_i \epsilon_i}{F_1 \epsilon_1} \tag{29}$$

we can write:

$$F_i\epsilon_i = \delta_i \sum_{j=1}^{i-1} F_j\epsilon_j = \delta_i\big(\sum_{j=1}^{i-2} F_j\epsilon_j + F_{i-1}\epsilon_{i-1}\big) = \delta_i\big(\sum_{j=1}^{i-2} F_j\epsilon_j + \delta_{i-1}\sum_{j=1}^{i-2} F_j\epsilon_j\big) = \delta_i(1+\delta_{i-1})\sum_{j=1}^{i-2} F_j\epsilon_j \tag{30}$$

By performing this operation $i-2$ times and arbitrarily setting $\delta_1 = 0$, we obtain:

$$F_i\epsilon_i = \delta_i \prod_{j=1}^{i-1}(1+\delta_j)F_1\epsilon_1 \quad \text{for } i = 2, \cdots, M \tag{31}$$

Code and data availability. We provide a simple implementation of the method in python within a Jupyter Notebook that includes the data used in this paper for illustration purposes.

Competing interests. The authors declare that they have no conflict of interest.

Acknowledgements. The work leading to the results presented here was supported by the People Programme (Marie Curie Actions) of the European Union's Seventh Framework Programme FP7/People/2012/ITN, Grant agreement number 316966.

~~Bernet, M., Brandon, M., and Garver, J. I. (2004). Downstream changes of Alpine zircon fission-track ages in the Rhône and Rhine Rivers. J. Sed. Res., 74:82–94.~~

~~Bracciali, L., Parrish, R. R., Najman, Y., Smye, A., Carter, A., and Wijbrans, J. R. (2016). Plio-Pleistocene exhumation of the eastern Himalayan syntaxis and its domal 'pop-up'. Earth Sc. Rev., 160(C):350–385.~~

~~Brandon, M. (1992). Decomposition of fission-track grain-age distributions. Am. J. Sci., 292:535–564.~~

~~Braun, J. (2016). Strong imprint of past orogenic events on the thermochronological record. Tectonophysics, 683:325–332.~~

~~Brewer, I. D., Burbank, D. W., and Hodges, K. V. (2006). Downstream development of a detrital cooling-age signal: Insights from 40Ar/39Ar muscovite thermochronology in the Nepalese Himalaya. In Special Paper 398: Tectonics, Climate, and Landscape Evolution, pages 321–338. Geological Society of America.~~

~~Brown, R. (1991). Backstacking apatite fission track "stratigraphy": a method for resolving the erosional and isostatic rebound components of tectonic uplift histories. Geology, 19:74–77.~~

~~Dodson, M. (1973). Closure temperature in cooling geochronological and petrological systems. Contrib. Mineral. Petr., 40:259–274.~~

~~Enkelmann, E. and Ehlers, T. A. (2015). Evaluation of detrital thermochronology for quantification of glacial catchment denudation and sediment mixing. Chemical Geology, 411(C):299–309.~~

~~Gleadow, A. and Brooks, C. K. (1979). Fission track dating, thermal histories and tectonics of igneous intrusions in East Greenland. Contributions to Mineralogy and Petrology, 71(1):45–60.~~

Hames, W. and Bowring, S. (1994). An empirical evaluation of the argon diffusion geometry in muscovite. Earth Planet. Sc. Lett., 124:161–169.

Lang, K. A., Huntington, K. W., Burmester, R., and Housen, B. (2016). Rapid exhumation of the eastern Himalayan syntaxis since the late Miocene. Geol. Soc. Am. Bull., 128:1403–1422.

Malusà, M. G., Resentini, A., and Garzanti, E. (2016). Hydraulic sorting and mineral fertility bias in detrital geochronology. Geol. Rundsch., 31:1–19.

McPhillips, D. and Brandon, M. (2010). Using tracer thermochronology to measure modern relief change in the Sierra Nevada, California. Earth Planet. Sc. Lett., 296:373–383.

Ruhl, K. W. and Hodges, K. V. (2005). The use of detrital mineral cooling ages to evaluate steady state assumptions in active orogens: An example from the central Nepalese Himalaya. Tectonics, 24(4):TC4015, doi:10.1029/2004TC001712.

Stock, G. M., Ehlers, T. A., and Farley, K. A. (2006). Where does sediment come from? Quantifying catchment erosion with detrital apatite (U-Th)/He thermochronometry. Geology, 34(9):725–728.

Vermeesch, P. (2007). Quantitative geomorphology of the White Mountains (California) using detrital apatite fission track thermochronology. J. Geophys. Res., 112(F3):FO3004.

Whipp, D. M., Ehlers, T. A., Braun, J., and Spath, C. D. (2009). Effects of exhumation kinematics and topographic evolution on detrital thermochronometer data. J. Geophys. Res., 114(F4):F04021.

Wobus, C. W., Hodges, K. V., and Whipple, K. X. (2003). Has focused denudation sustained active thrusting at the Himalayan topographic front?Geology, 31:861864.

Wobus, C. W., Whipple, K. X., and Hodges, K. V. (2006). Neotectonics of the central Nepalese Himalaya: Constraints from geomorphology, detrital 40Ar/ 39Ar thermochronology, and thermal modeling. Tectonics, 25(4):TC4011.

References

Bernet, M., Brandon, M., and Garver, J. I.: Downstream changes of Alpine zircon fission-track ages in the Rhône and Rhine Rivers, J. Sed. Res., 74, 82–94, 2004.

Bracciali, L., Parrish, R. R., Najman, Y., Smye, A., Carter, A., and Wijbrans, J. R.: Plio-Pleistocene exhumation of the eastern Himalayan syntaxis and its domal 'pop-up', Earth Sc. Rev., 160, 350–385, 2016.

Brandon, M.: Decomposition of fission-track grain-age distributions, Am. J. Sci., 292, 535–564, 1992.

Braun, J.: Strong imprint of past orogenic events on the thermochronological record, Tectonophysics, 683, 325–332, 2016.

Brewer, I. D., Burbank, D. W., and Hodges, K. V.: Downstream development of a detrital cooling-age signal: Insights from 40Ar/39Ar muscovite thermochronology in the Nepalese Himalaya, in: Special Paper 398: Tectonics, Climate, and Landscape Evolution, pp. 321–338, Geological Society of America, 2006.

Brown, R.: Backstacking apatite fission track "stratigraphy": a method for resolving the erosional and isostatic rebound components of tectonic uplift histories, Geology, 19, 74–77, 1991.

Dodson, M.: Closure temperature in cooling geochronological and petrological systems, Contrib. Mineral. Petr., 40, 259–274, 1973.

Enkelmann, E. and Ehlers, T. A.: Evaluation of detrital thermochronology for quantification of glacial catchment denudation and sediment mixing, Chemical Geology, 411, 299–309, 2015.

Enkelmann, E., Ehlers, T. A., Zeitler, P. K., and Hallet, B.: Denudation of the Namche Barwa antiform, eastern Himalaya, Earth Planet. Sc. Lett., 307, 323–333, 2011.

Garzanti, E. and Andò, S.: Heavy mineral concentration in modern sands: implications for provenance interpretation, pp. 567–598, Elsevier, Amsterdam, 2007.

Gemignani, L., Sun, X., Braun, J., van Geerve, D., Thomas, R., and Wijbrans, J.: A new detrital mica $^{40}Ar/^{39}Ar$ dating approach for provenance and exhumation of the Eastern Alps, Tectonics, 36, 1521–1537, 2017.

Gleadow, A. and Brooks, C. K.: Fission track dating, thermal histories and tectonics of igneous intrusions in East Greenland, Contributions to Mineralogy and Petrology, 71, 45–60, 1979.

Hames, W. and Bowring, S.: An empirical evaluation of the argon diffusion geometry in muscovite, Earth Planet. Sc. Lett., 124, 161–169, 1994.

Kellett, D. A., Grujic, D., Coutand, I., Cottle, J., and Mukul, M.: The South Tibetan detachment system facilitates ultra rapid cooling of granulite-facies rocks in Sikkim Himalaya, Tectonics, 32, 252–270, 2013.

Lang, K. A., Huntington, K. W., Burmester, R., and Housen, B.: Rapid exhumation of the eastern Himalayan syntaxis since the late Miocene, Geol. Soc. Am. Bull., 128, 1403–1422, 2016.

Malusà, M. G., Resentini, A., and Garzanti, E.: Hydraulic sorting and mineral fertility bias in detrital geochronology, Geol. Rundsch., 31, 1–19, 2016.

McPhillips, D. and Brandon, M.: Using tracer thermochronology to measure modern relief change in the Sierra Nevada, California, Earth Planet. Sc. Lett., 296, 373–383, 2010.

Resentini, A. and Malusà, M. G.: Sediment budgets by detrital apatite fission-track dating (Rivers Dora Baltea and Arc, Western Alps), Geol. Soc. Am. Spec. Pap., 487, 125–140, 2012.

Ruhl, K. W. and Hodges, K. V.: The use of detrital mineral cooling ages to evaluate steady state assumptions in active orogens: An example from the central Nepalese Himalaya, Tectonics, 24, TC4015, doi:10.1029/2004TC001 712, 2005.

Sambridge, M. and Compston, W.: Mixture modeling of multi-component data sets with application to ion-probe zircon ages, Earth Planet. Sc. Lett., 128, 373–390, 1994.

Singh, S. and France-Lanord, C.: Tracing the distribution of erosion in the Brahmaputra watershed from isotopic compositions of stream sediments, Earth Planet. Sc. Lett., 202, 2002.

Stewart, R., Hallett, B., Zeitler, P., Malloy, M., Allen, C., and Trippett, D.: Brahmaputra sediment flux dominated by highly localized rapid erosion from the easternmost Himalaya, Geology, 36, 711–714, 2008.

Stock, G. M., Ehlers, T. A., and Farley, K. A.: Where does sediment come from? Quantifying catchment erosion with detrital apatite (U-Th)/He thermochronometry, Geology, 34, 725–728, 2006.

Vermeesch, P.: Quantitative geomorphology of the White Mountains (California) using detrital apatite fission track thermochronology, J. Geophys. Res., 112, FO3004, 2007.

Vermeesch, P.: On the visualisation of detrital age distributions, Comput. Geosci., 312, 190–194, 2012.

Whipp, D. M., Ehlers, T. A., Braun, J., and Spath, C. D.: Effects of exhumation kinematics and topographic evolution on detrital thermochronometer data, J. Geophys. Res., 114, F04 021, 2009.

Wobus, C. W., Hodges, K. V., and Whipple, K. X.: Has focused denudation sustained active thrusting at the Himalayan topographic front?, Geology, 31, 861864, 2003.

Wobus, C. W., Whipple, K. X., and Hodges, K. V.: Neotectonics of the central Nepalese Himalaya: Constraints from geomorphology, detrital 40Ar/ 39Ar thermochronology, and thermal modeling, Tectonics, 25, TC4011, 2006.

Yin, A., Dubey, C., Kelty, T., Webb, A., Harrison, T., Chou, C., and Célérier, J.: Geologic correlation of the Himalayan orogen and Indian craton: Part 2. Structural geology, geochronology, and tectonic evolution of the Eastern Himalaya, Geol. Soc. Am. Bull., 122, 360–395, 2010.